Single-cell RNA-seq Reveals Early Transcriptional Programs of the Maternal to Zygote Transition in Mice and Rats

Yangqi Su[1], Evguenia Kouranova[2], Jonathan Shea[1], Xiaoxia Cui[2]* and Zhengchang Su[1]*

[1]Department of Bioinformatics and Genomics, the University of North Carolina at Charlotte, Charlotte, NC 28223, USA

[2]Department of Genetics, Washington University in St. Louis, St. Louis, MS, USA

* To whom correspondence should be addressed: zcsu@uncc.edu and x.cui@wustl.edu

Abstract

The maternal to zygote transition in mammals has been an area of intensive research over the past few decades, with an ever-changing landscape of understanding that has accompanied the rapid development of cell-profiling technology. Utilizing a full-length single cell RNA-seq protocol, we profiled mature oocytes and zygotes of mice and rats to uncover elusive transcriptomic dynamics during the maternal to zygote transition. We confirm the existence of early gene expression in the mouse zygote while revealing a similar chain of events occurring in the rat zygote. We observe an increase in nascent transcription in both species. Moreover, we find subtle but pervasive signals of differential splicing of genes related to key early zygotic activities occurring in both species. Meanwhile, we find distinct profiles of alternative polyadenylation between zygotes and oocytes in both species, particularly, in genes related to major processes within the zygotes. Finally, although a more dynamic transcriptomic landscape exists in the mouse zygote, the rat zygote also displays similar transcriptomic features, suggesting that minor zygotic activation in rat occurs earlier than originally thought.

Keywords: mouse, rat, ZGA, MZT, scRNA-seq

Introduction

Fusion of the oocyte and sperm forming the zygote marks the inception of all mammalian embryogenesis, during which the male and female genome come together to jumpstart the developmental process(McGrath & Solter, 1984). Despite providing half the DNA and being crucial for oocyte activation, the sperm brings few components in the zygote, and thus provides smaller sources in the early stages of embryogenesis than the oocyte. It is therefore mainly the contents of the maternal gamete that set up the suitable environment for successful polyspermy prevention and zygote genome activation (ZGA). During ZGA the control of cellular processes is gradually let go mainly from the products of the maternal genome and transferred to products of the zygote genome(Saunders et al., 2002; Sutovsky & Schatten, 2000). This process, also known as maternal to zygote transition (MZT) (Tadros & Lipshitz, 2009), has long been the subject of interest for researchers. Most foremost, the oocyte is a highly differentiated cell that quickly acquires pluripotency after fertilization. Though much research has been conducted in this area, it is still an elusive topic, and many intricacies remain to be uncovered.

An aspect that has been observed in MZT of all mammals has been the silence of the transcriptome in mature oocytes prior to fertilization up until ZGA after fertilization, which initiates the events of embryogenesis(Lee et al., 2014). The length of this period of transcriptional silence varies in different species. This quiescent period that is conserved among species has not been fully understood, particularly, the mechanisms underlying ZGA may be different for each species(Schulz & Harrison, 2019). Nonetheless, in all the mammalian species the machineries that carry on the progression of meiosis and remodel the genome depend solely on the maternal mRNAs accumulated during oocyte development(Lee et al., 2014; Schulz & Harrison, 2019). Thus

prior to ZGA, there is also translation and degradation of many maternal mRNAs(Ma et al., 2013; Sha et al., 2020).

The mouse (*Mus musculus*) and rat (*Rattus norvegicus*) are two of the most used model mammals in biomedical research. Many aspects of the two organisms are very similar, such as genome size and number of protein-coding genes. It is estimated that at least 90% of genes in the mouse genome have at least a homolog in the rat genome, and vice versa (Srivastava et al., 2020). However, there remain considerable differences in the biology of the two organisms including reproduction(Mullins & Mullins, 2004). For instance, it is known that ZGA occurs in 2 waves in mice with a 'minor ZGA' in the late 1-cell stage and a 'major ZGA' in 2-cell stage. In contrast, it was reported that the onset of embryonic transcription activity in rats occur in late 2-cell stage(Abe et al., 2018; Zernicka-Goetz, 1994). However, even though major ZGA is known to occur at the 8-cell stage in human embryos, recent research has suggested that minor ZGAs occur in 1-cell human zygotes as well, though to a lesser degree than that of mice(Xue et al., 2013). Thus, it is possible that similar transcriptional events might also occur in 1-cell rat zygote.

Research into transcriptional events occurring during minor ZGA in mice has revealed insightful results. Early studies in mice using brUTP incorporation found that transcription occured in the S stage of 1-cell zygote, and transcription of MUREV (define the acronym) genes was verified via RT-PCR studies (Aoki et al., 1997). Another study found that transcription was promiscuous across open chromatin regions of the mouse zygote genome, with many transcripts containing intronic and intergenic regions, indicating limited 3'end processing and splicing mechanisms involved, possibly to protect the zygote from precocious gene expression(Abe et al., 2018).

Although the understanding of transcriptional events in the zygote is still inconclusive in many species, post-transcriptional regulation of transcripts appears to be ubiquitous. A pivotal aspect of post-transcriptional modification is cleavage and polyadenylation of maternal mRNAs. The choice of polyadenylation cleavage sites in 3' untranslated regions (3' UTRs) is thought to influence various UTR binding components that in turn regulate the stability, translation, and degradation of transcripts. Post-transcriptional regulation via alternative poly-A cleavage sites as well as the length of poly-A tail plays vital roles in MZT in many organisms. For example, poly-A tail lengthening promotes global translation in *Drosophila* zygotes (Eichhorn et al., 2016). Removal of de-adenylation components in mouse oocytes leads to developmental arrest in pre-implantation embryos (Liu et al.; Pasternak et al.; Sha et al.). A recent study has also found extensive remodeling of maternal mRNAs in human embryos via poly-A tail modifications such as changes in poly-A tails and 3'UTR lengths, which are essential for MZT in humans (Liu et al., 2023).

Furthermore, despite the plethora of studies into the embryonic development of mice, little is known about the maternal vs zygote transcriptomic landscape in rats, and how the shared and differing characteristics with mice contribute to early stages of their respective pre-implantation embryos. The rise in application of single-cell transcriptomic studies has opened a front into studying the intricacies of developmental dynamics at the single-cell level. However, many such transcriptomic studies overlook alternative insights that can be made apart from gene expression. In this study, we present orthogonal forms of comparative analysis on the transcriptomic landscape of the early MZT by applying a full-length single-cell RNA sequencing (scRNA-seq) protocol (Picelli et al., 2013) to oocytes and zygotes in mice and rats. We identify RNA transcripts that are

produced, modified, or degraded in the zygotes. We also reveal mechanisms that are unique and conserved in the two species.

Materials and Methods

Harvest and preparation of oocytes and zygotes

Mouse and rat oocytes and zygotes were isolated at Horizon Discovery, St. Louis site, operated under approved animal protocols overseen by Horizon Discovery's Institutional Animal Care and Use Committee (IACUC). C57BL/6N mice and Sprague Dawley rats purchased from Taconic Farms were housed in standard cages and maintained on a 12-h light/dark cycle with *ad libitum* access to food and water. Three- to four-week-old female mice were injected with PMS (5 IU/mouse) 48 hr before hCG (5 IU/mouse) injection, followed by with or without mating to stud males. Fertilized eggs and oocytes were harvested 1 d later, respectively. Four- to five-week-old female rats were injected with 20 units of PMS, which was followed by an injection of 50 units of hCG 48 h later, followed by with or without mating to stud males. Fertilized eggs and oocytes of both species were harvested 1 d later.

Construction of scRNA-seq libraries

Full-length double-strand cDNA for each oocyte or zygote was prepared using an sc-RNA-seq libraries SMART-Seq v4 Ultra Low Input RNA Kit (Clontech, Mountain View, CA) following the vendor's instruction, which was based on the Smartseq2 protocol (Picelli et al., 2013). cDNA-seq libraries were constructed using a Nextera® XT DNA Library Preparation Kit (Illumina, Sandiago, CA, Cat. Nos. FC-131-1024, FC-131-1096) following the vendor's instruction. The libraries were quantified using an Agilent 2100 Bioanalyzer (Agilent Technologies, Santa Clara) and sequenced on an Illumina 2500 machine with 150 bp paired end reads.

Transcriptome mapping and quantification

The mouse genome assembly (GCF_000001635.27) with annotation version GRCm39 and the rat genome assembly (GCF_015227675.2) with annotation version mRatBN7.2 were obtained from NCBI Genbank. Raw sequences were trimmed using Trim_galore (Krueger, 2015), with parameters length > 35 and q > 10, and subsequently mapped to the respective reference genome using HISAT2(Kim et al., 2019) with default settings. The resulting mappings were quantified using HTSeq (Anders et al., 2015) with default settings to obtain read counts. Trimmed reads were also mapped to the respective reference genome using Salmon(Patro et al., 2017) with default settings to obtain expression levels in per million (TPM) for both genes and transcripts. Quantification of read coverage of nascent transcripts was performed using kallisto(Bray et al., 2015)/bustools (Melsted, Ntranos, et al., 2019) in the kb_python package (v0.28.0) (Melsted, Booeshaghi, et al., 2019; Sullivan et al., 2023). More specifically, trimmed reads were aligned to the reference genome with kb_python under the 'nac' workflow with default settings.

Quality control and exploratory analysis

Samples with more than 5% reads mapped to rRNA genes or 25% reads mapped to the mitochondrial genome were removed from further analysis. Furthermore, only genes whose biotypes belong to protein-coding, lncRNA and transcribed pseudogenes were kept for further analysis. Samples were visualized using Uniform Manifold Approximation and Projection (UMAP) based on log transformed DESeq(Love et al., 2014) median normalized counts, outliers were filtered out for further analysis .

Differentially expressed gene (DEG) analysis

Due to the inherent high variability intrinsic to single cell transcriptomic data, to ensure genes had sufficient coverage and replicates for DEG analysis**,** we only considered genes that were expressed

in at least 6 samples. DEG analysis of both mouse and rat samples were carried out with count values from HISAT2(Kim et al., 2019)/(Anders et al., 2015). The raw counts were normalized to Counts per Million (CPM) and log transformed prior to analysis with MAST (Finak et al., 2015). In fitting the data to the MAST model, we enabled the useContinuousBayes option to estimate $\log_2$(foldchange) values for genes that had no expression in oocytes or zygotes. For each species, genes with an FDR < 0.05 and a foldchange greater than 2 or less than 0.5 were considered differentially expressed.

Estimation of pre-mature mRNA transcripts

Estimation of nascent mRNA transcripts was carried out through kallisto/bustools (Melsted, Ntranos, et al., 2019; Sullivan et al., 2023) using the kb_python (version = 0.28) wrapper, with method = 'nac'. The method is based on the idea that the number of nascent mRNAs for each gene inside the cell reflects a snapshot in the cell's transcription dynamics, and thus by inferring nascent and mature mRNA levels for many cells, it is possible to delineate developmental trajectories by modeling the RNA production using differential equations. From henceforth, we shall use the terms un-spliced reads, nascent reads and intronic reads interchangeably to describe the reads that cover intronic portions of genes. A gene was considered to have pre-mature mRNA expression if it met the following criteria:

- mean read coverage of spliced transcripts across either zygote or oocyte samples > 5.
- spliced transcripts were expressed in 10% of either zygote or oocyte samples.
- mean read coverage of un-spliced transcripts across either zygote or oocyte samples > 0.
- un-spliced transcripts expressed in 10% of either zygote or oocyte samples.
- R^2 of linear model fit between spliced and un-spliced reads of all samples > 0.1.
- Kendall correlation between spliced and un-spliced reads of all samples > 0.1.

- Ratio of standard deviation of spliced reads over standard deviation of un-spliced reads was between 0.005 and 5.

This filtering criteria was set to ensure that estimation of nascent read coverage truly came from un-spliced intronic portions of transcripts. DEG analysis of un-spliced genes was performed with MAST, with un-spliced reads normalized by sample-wise CPM normalization factors used in the DEG analysis. We define the nascent proportion of a gene as the ratio of the mean spliced read coverage over the mean un-spliced read coverage in a cell. To test differences in nascent proportions (DNP) of a gene between zygotes and oocytes, we applied a Fisher's exact test.

Differential transcript usage (DTU) analysis

DTU analyses were performed under the guidelines given by (Love et al., 2018). Specifically, transcript abundances (TPM values) estimated by Salmon(Patro et al., 2017) were first filtered using Drimseq(Nowicka & Robinson, 2016) with default parameters. The filtered data was then analyzed using DEXseq(Anders et al., 2012) with default settings. Instead of exons in the original applications (Anders et al., 2012), each transcript of a gene was regarded as an exon in our case. The DEXseq results for each gene were aggregated and further analyzed using stageR(Van Den Berge et al., 2017) to determine if it exhibited DTU while overall false discovery rate was controlled on the gene level.

Alternative polyadenylation analysis

HISAT2 aligned BAM files were first filtered using samtools(Li et al., 2009) to only include concordantly and uniquely mapped reads. The resulting filtered bam files were then transformed into BEDGRAPH format using bedtools(Quinlan & Hall, 2010). Custom scripts were used to account for the pair-end and spliced natures of the read mappings. Primary lists of mouse and rat

3'UTRs were obtained by extracting 3'UTRs from the NCBI annotation files and only unique 3'UTRs were kept. A secondary list of 3'UTRs in each species was obtained using DaPars2 (Feng et al., 2018; Wang et al., 2014) following the authors' instructions. The 3'UTRs in the secondary list may include coding sequences in the last exon. Thus, if the 3'UTRs in the primary and secondary lists of a species were from the same isoform, only the one in the primary list was kept. Though most UTRs were composed of a single continuous segment, there was still a significant portion of UTRs that contained introns. In these cases, we discarded all segments with length < 150 bp and treated the remaining ones as individual 3'UTRs. We identified genes with differential alternative polyadenylation (DAP) in each species using DaPars2 (Feng et al., 2018; Wang et al., 2014), which computed a Percentage of Distal poly-A site Usage Index (PDUI) by de novo estimating putative polyadenylation breakpoints via read coverage change on the lists of 3'UTRs. To ensure more accurate DAP analysis, we modified DaPars2 as follows:

1. Searching for breakpoints 25 bp instead of the default 150 bp downstream of the 3'UTR start point and only analyzed 3'UTRs > 150 bp.
2. Furthermore, instead of using read depth of each sample for normalization, we used DESeq2-estimated size factor of each sample's read counts as normalization factor.
3. Allowing DaPars2 to produce distal and proximal polyadenylation site coverages in addition to PDUI units for each UTR.

Moreover, the threshold for coverage was set to 0, thus, any read coverage was counted in the estimation of alternative polyadenylation. Prior to testing, we filtered out genes with less than 10 reads detected in any of the samples, as well as genes with no coverage in both distal and proximal 3'UTRs (PDUI == 'NA') in more than 5 samples. We then performed Fisher's exact test to evaluate the differences in distal vs proximal polyadenylation preference between oocytes and

zygotes using mean distal/proximal coverage in oocyte and zygote samples. Differences in mean PDUI between oocytes and zygotes were also calculated. To aggregate the results to gene level (many genes have multiple 3'UTRs), for each gene, we selected the UTR with the lowest p-value. If multiple different UTRs of a gene had a tied p-value, the one with the largest absolute difference in PDUI was chosen. The resulting p-values were then controlled for false discovery rate with the qvalue package in R. Finally, genes with UTRs that had an absolute mean expression difference > 0.2 and a false discovery rate < 0.05 were considered to have differential alternative polyadenylation. Gene-body coverage in each sample was normalized by the BEDGRAPH coverage as aforementioned, and the average was taken over the oocyte or zygote samples. The normalized BEDGRAPH coverage was processed and visualized using custom scripts and the trackViewer R package(Ou & Zhu, 2019).

Pathway and GO term enrichment analysis

The ClusterProfiler(Yu et al., 2012) R package was used to perform both gene set enrichment analysis and over-representation analysis with gene sets from KEGG (Kanehisa et al., 2022; Kanehisa & Goto, 2000), Gene Ontology Biological Processes (GO BP)(Gene Ontology, 2021), Reactome (Milacic et al., 2024) and Wikipathways(Martens et al., 2021).

Analysis of orthologs between mouse and rat

Orthologs between mice and rats were obtained from the MGI database(Blake et al., 2021). Specifically, rat and mouse genes belonging to the same homology class were considered as orthologs. Over-representation analysis was performed on orthologous genes that had an absolute foldchange > 1.25 at an FDR < 0.05 in both species with all orthologous genes that were tested for differential expression in both species as the background set. The analysis was based on mouse gene annotations in the GO BP, KEGG, Reactome and Wikipathways databases. Visualization of

gene networks was generated using clusterProfiler(Yu et al., 2012). All intersections of genes with DNP, DTU and DAP were performed with the respective results obtained in the prior analysis. All gene coverage plots were generated via the trackViewer(Ou & Zhu, 2019) package.

Results

Oocytes and zygotes of both mice and rats display distinct transcriptomic patterns

We sequenced the transcriptomes of a total of 17 mouse oocytes, 17 mouse zygotes, 15 rat oocytes, and 16 rat zygotes, with an average of 10,018,474 pairs of reads/cell (Table S1). The vast majority (>90%) of the reads could be mapped to the respective genomes for most (53/81.52) samples (Table S1). However, 6 mouse oocytes, 1 rat oocyte and 5 rat zygotes exhibited high levels of reads mapping to mitochondrial or ribosomal genes, we thus excluded them from further analyses (Table S1) (Materials and Methods). This left us with 28 mouse samples (11 oocytes / 17 zygotes) and 25 rat samples (14 oocytes and 11 zygotes). Interestingly, the reads from mouse samples, particularly, from mouse oocytes, were strongly biased to the 3' ends of CDSs of genes, while the bias was not seen in both rat oocytes and zygotes (Figure S1A). We detected transcripts for an average of 14,514 and 15,934 annotated genes in mouse oocytes and zygotes, respectively, and for an average of 12,826 and 13,535 annotated genes in rat oocytes and zygotes, respectively (Figure S1B). Thus, there were more genes expressed in zygotes than in oocytes of both species. Furthermore, oocytes and zygotes of both species are clearly separated by estimated gene expression levels in UMAP displays (Figures 1A, 1B), indicating that oocytes and zygotes of both mice and rats contain distinct sets of gene transcripts.

ZGA in rats may begin earlier than previously believed

We first compared expression levels of genes in zygotes relative to those in oocytes of each species. We found 4,603 DEGs in mice, but only 842 DEGs in rat (Figure 1C). Of the mouse DEGs, a smaller portion (1,368 or 29.7%) were upregulated while the remaining larger portion (3,235 or 70.3%) were downregulated (Figure 1C). In contrast, of the rat DEGs, a larger portion (627 or 74.5%) were upregulated while the remaining smaller portion (215 or 25.5%) were downregulated (Figure 1C). Since the zygotes of both species were analyzed prior to the first cell division, the elevated transcriptional activities of the 1,368 upregulated DEGs in mice might reflect the previously reported initial transcriptional events in the mid-1cell stage zygote(Abe et al., 2018; Schultz, 1993) . Interestingly, even though at a smaller scale, the elevated transcriptional activities of the 627 upregulated DEGs in rats might unveil an early wave of transcriptional activation in rat zygotes, which was previously believed to not occur until later stage of embryogenesis (Zernicka-Goetz, 1994).

Distinct pathways are up- or down-regulated in both mouse and rat zygotes

Downregulated genes in mouse zygotes were significantly enriched for GO BP or pathways including cytoplasmic translation, rRNA processing, nonsense-mediated decay, TCA cycle, energy production and chromatin modifying enzymes, etc. (Figures 1D, 2A). For example, ribosomal protein subunits encoding genes such as *Rpl*3/9/12/18/19/26 (Nakao, 2004) were downregulated in mouse zygotes (Figure 1D), a result that is in excellent agreement with the earlier findings (Schultz et al., 1979). Genes that function in the TCA cycle *such as Ndufa2/Nudfb7/Ndufa8/Ndufc1* (Vinothkumar et al., 2014) and genes involved in energy production such as *Atpa1a/Atp5h* (Song et al., 2018) showed decreased transcript levels (Figure 1D). On the other hand, upregulated genes in mouse zygotes were significantly enriched for biological processes or pathways including mRNA transport, cell cycle, transcription, DNA

replication, energy production, etc. (Figures 1D, 2A). For instance, genes *Pdhb, Pdp1, Pdhx* and *Dlat* were upregulated, which encode components of the pyruvate dehydrogenase complex responsible for acetyl-CoA biosynthesis from pyruvate (Zhou et al., 2001)(Figures 1D). Interestingly, the role of the TCA cycle in ZGA was previously studied in early mouse embryos, and it was found that despite low metabolic requirements in early embryo, pyruvate was responsible for the nuclear localization of several TCA enzymes that might contribute to epigenetic regulations that were essential for major ZGA activation in the 2-cell stage(Nagaraj et al., 2017). RNA polymerase II subunit genes *Taf*6/9 (Cler et al., 2009; Juven-Gershon et al., 2008), cell cycle genes *Cdc20, Mastl, Mad2l1*and *Ube2e1*(Guo et al., 2020; Rogers et al., 2018; Wheaton et al., 2017; Wu et al., 2017), and general transcription factor II genes *Gtf2a2/2b*(Roeder, 1996) also exhibited upregulation in mouse zygotes (Figure 1D). Genes *Nup35/37/54* encoding nucleoporin (Nup), and gene *Nxt1* encoding the nuclear transport factor 2-like export factor (Xie & Ren, 2019) were upregulated, suggesting increased transport of mRNA and proteins between the nucleus and cytoplasm in mouse zygotes, in line with recent findings that knockdown of the nucleoporin gene *Nup37* led to reduced blastocyte formation rates (Guo et al., 2022) and that massive remodeling of the nuclear envelope occurred during minor zygotic activation in bovine pre-implantation embryos (Popken et al., 2015). Moreover, we found genes encoding essential ZGA transcription factors *Obox1/2/5/7* were all upregulated in mouse zygotes (Figure 1D), suggesting that the elevation of transcription levels of these genes during minor ZGA may also be at least partially transcriptional and not solely of maternal origin as reported by a recent study (Ji et al., 2023).

Downregulated genes in rat zygotes were enriched for biological processes or pathways including non-sense mediated decay, RNA polymerase 1 promotor opening, structural constituent of chromatin, etc. (Figure 1E, 2B). For instance, as in the case of mouse zygotes, genes encoding

ribosomal proteins also were downregulated in rat zygotes (Figure 1E, 2B). Moreover, Genes *NuRD* and *CHD* involved in chromatin remodeling were down-regulated (Figure 1E). Upregulated genes in rat zygotes were enriched for four biological processes or pathways including carbon metabolism and the TCA cycle, etc. For instance, transcription of the following genes involved in the TCA cycle were all upregulated in rat zygotes: *Aco2* (aconitase 2) (Ciccarone et al., 2017), *Pdha1*(pyruvate dehydrogenase component) (Zhou et al., 2001), *Idh1* (pyruvate dehydrogenase) (Ni et al., 2022), *Sdhc*/d (succinate dehydrogenase subunits) (Rutter et al., 2010), and *Dlst* (dihydrolipoamide S-succinyltransferase) (Berg et al., 2002)(Figure 1E). This result contrasts with that seen in mouse zygotes where some TCA cycle genes were downregulated while some others were upregulated (Figures 1D, 2A). Coupled with the aforementioned studies showing that several TCA cycle enzymes were transiently localized in the nucleus of mammalian embryos and essential for major ZGA (Kafkia et al., 2022; Nagaraj et al., 2017), the shared increased expression of the said enzymes in both species suggests that these enzymes may be regulated at the transcriptional

level during minor ZGA. Taken together, these results once more suggest that ZGA in the rat might begin earlier than previously believed.

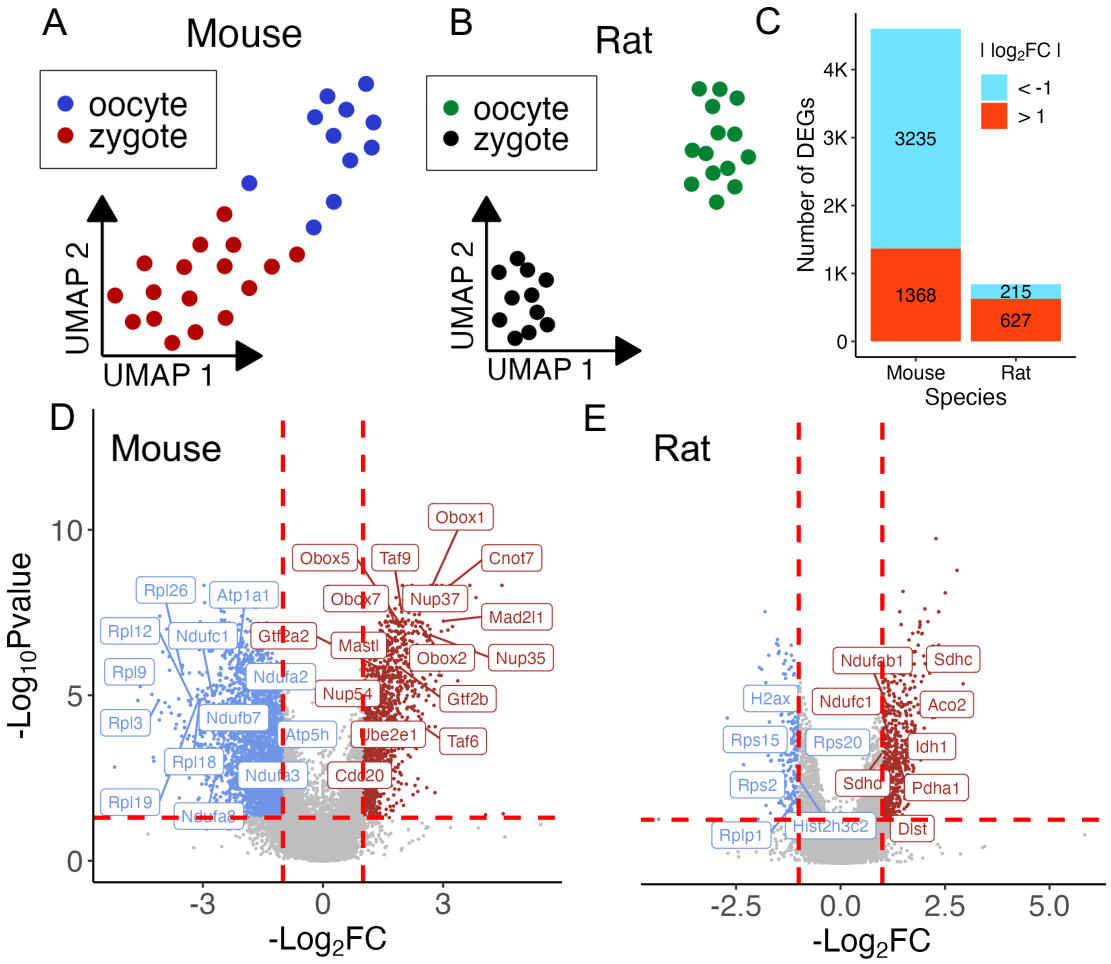

Figure 1. Oocytes and zygotes of both species contains distinct sets of transcripts. A. UMAP visualization of single mouse oocytes and zygotes based on expression levels of genes. **B.** UMAP visualization of single rat oocytes and zygotes. **C.** Number of up- or down-regulated DEGs in mouse and rat zygotes relative to respective oocytes. **D, E.** Volcano plots of $-\text{Log}_{10}$Pvalues vs Log_2FC of mouse (D) and rat (E) genes. Genes marked red were significantly upregulated ($\text{Log}_2\text{FC} > 1$ and FDR < 0.05), while those marked blue were significantly downregulated ($\text{Log}_2\text{FC} < -1$ and FDR < 0.05) in zygotes relative to oocytes.

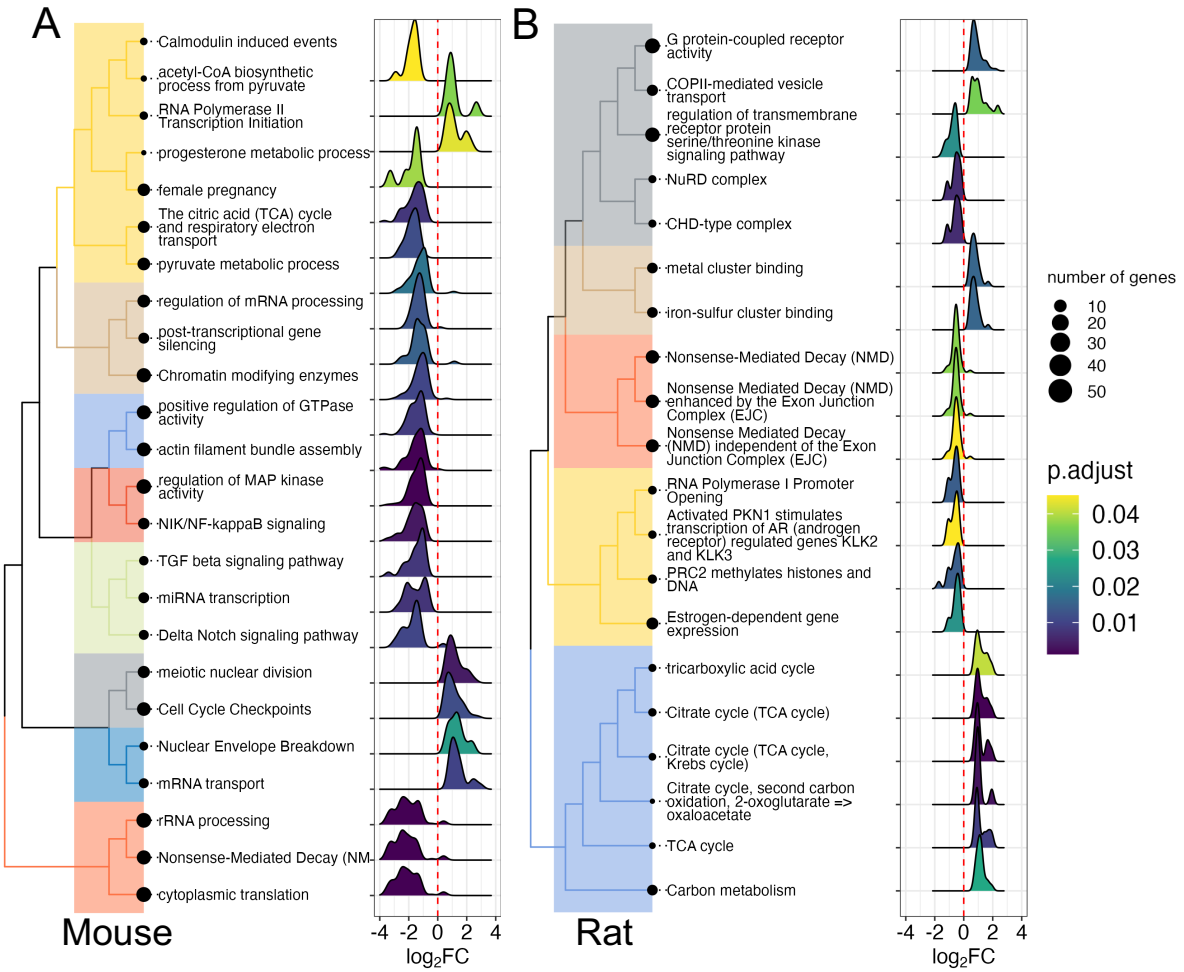

Figure 2 A, B. Enriched GO BP terms, Wikipathways, KEGG Pathways and Reactome at FDR < 0.05 in mouse (A) and rat (B). Significant pathways and gene sets are clustered into similar groups based on Jaccard's similarity for ease of viewing, density plots for each gene set/pathway show distribution of the $\log_2$FC of the genes in the indicated GO BP or pathways.

Pre-mature mRNA transcription is elevated in zygotes of both species

It has been reported that early transcriptional events in the zygote produced pre-mature (nascent) RNAs that originated from intronic as well as intergenic regions(Abe et al., 2015). We thus estimated nascent (un-spliced) and mature (spliced) transcripts in the samples of both species (Materials and Methods). We detected a total of 26,514 and 21,009 genes with read coverage in the mouse and rat oocytes and zygotes, of which 3,639 (13.8%) and 2903 (13.7%) had nascent

reads, respectively (Supplementary Figure 2A). In both species, zygotes contained higher proportions of nascent reads than oocytes (Figure 3B). We also quantified reads mapped to 1 kb binned intergenic regions as has been done previously(Abe et al., 2015). Zygotes in both species had significantly larger numbers of bins with >1 read coverage than oocytes (Figure 3C). These results confirm the previous findings of increased expression of nascent transcripts in 1-cell mouse zygotes, while also suggesting that a similar phenomenon of transcription occurs in the 1-cell rat zygotes. We then performed a DGE analysis of genes with nascent transcripts in oocytes and zygotes (Materials and Methods). As shown in Figure 3C, Log_2FC values of nascent transcripts and Log_2FC values of spliced transcripts are strongly correlation, indicating that nascent transcripts mostly change in the same ways as their spliced counterparts.

To identify genes that exhibited significant changes in the proportion of nascent transcripts, we performed a DNP analysis between oocytes and zygotes in both species (Materials and Methods). We found that mouse had more genes with decreased nascent proportions than with increased nascent proportions (113 vs 86), while rat had more genes with increased nascent proportions than with decreased nascent proportions (50 vs 35) (Figure 3D). Comparisons of DEGs and DNP genes in both species found only small overlaps between DEGs and DNPs (Figure 3E, 3F). However, in both species, the largest overlap was between upregulated DEGs and genes with decreased nascent proportions (Figure 3E, 3F). Although this was expected in rats due to a greater number of upregulated DEGs than downregulated DEGs (Figure 2C), it was surprising in mice, since mouse had many more down-regulated DEGs than upregulated DEGs (Figure 3E). This result suggests that some of upregulated DEGs in mice could be due in part to more mature transcripts in the zygote cytoplasm that could have been stored as unprocessed transcripts in the

oocyte nucleus. Over-representation analysis of these DNP genes in both species yielded no significant pathways or GO BP terms when accounting for false discovery rate. However, we found changes in genes that played important roles in either oocytes or zygotes. For instance, the nascent proportion of the *Oog1/2* genes increased in mouse zygotes (Figure 3G), which is known to be required for oocyte development (Minami et al., 2003; Monti & Redi, 2009). The nascent proportion of the *Obox* genes increased in mouse zygotes (Figure 3G), consistent with our earlier observation that the *Obox* genes were upregulated in the zygotes as a part of the minor ZGA process, albeit in unprocessed transcript form. The *Nlrp4b/g* genes also exhibited decreased nascent proportions in mouse zygotes (Figure 3G), in agreement with the previous reports that the *Nlrp* transcripts were maternally derived and played essential roles in zygotic genome (Chang et al., 2013; Li et al., 2015). Although DNP genes in rats were less evident, we found the *Zar1* gene to exhibit decreased nascent transcript proportion (Figure 3G), consistent with the previous report that Zar1 played essential roles in zygotic genome activation by regulating maternal derived RNAs (Wu et al.).

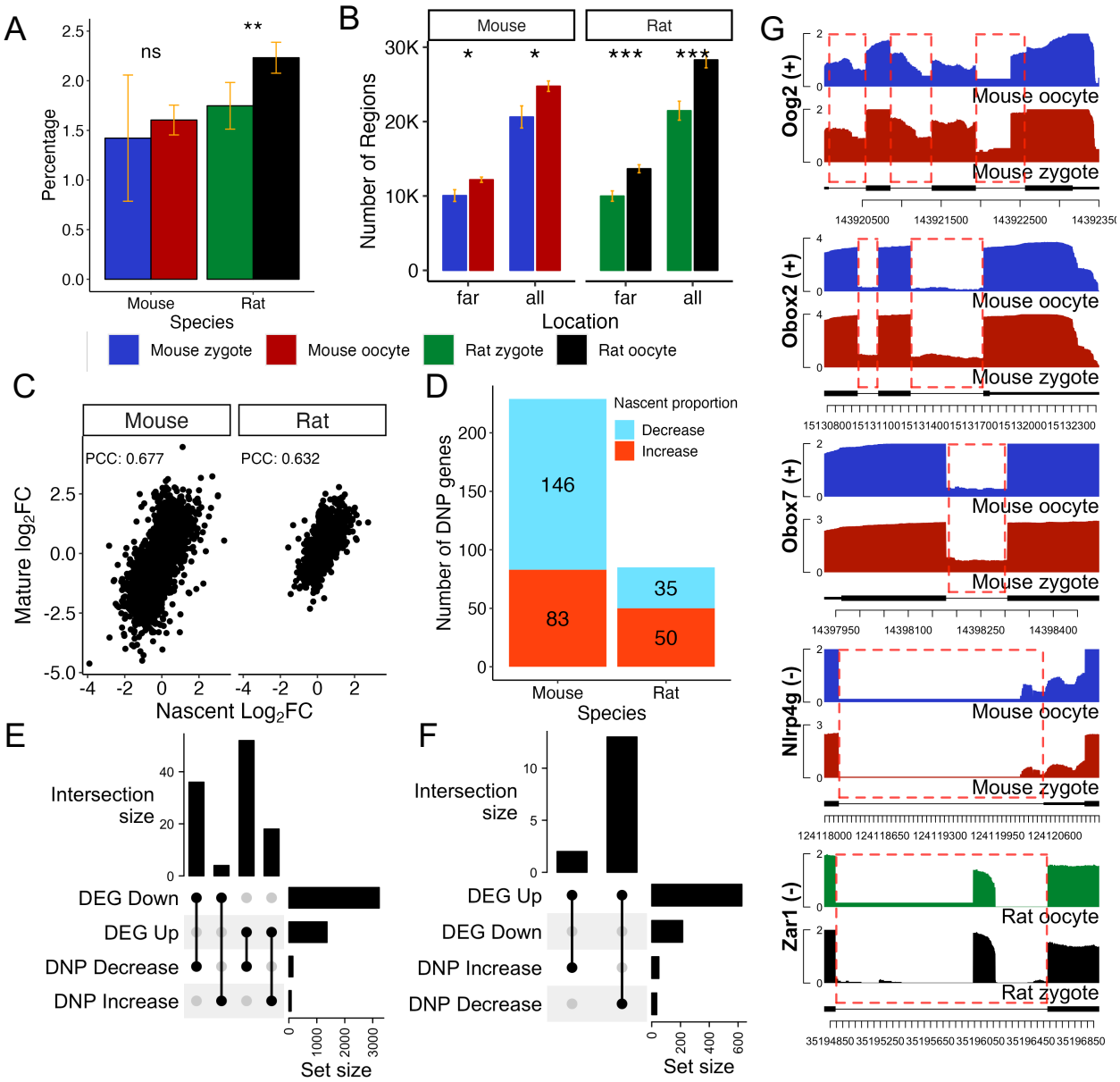

Figure 3. Expression of pre-mature mRNA transcripts in oocytes and zygotes of both species. **A.** Average percentage of total un-spliced reads out of all reads (spliced and un-spliced) in oocytes and zygotes of mice and rats. **B.** Number of all and far 1kb intergenic regions with reads in oocytes and zygotes of the two species. Far regions are >10kb downstream or upstream of any gene. **C.** Scatter plots of MAST estimated Log_2FC values of un-spliced reads and Log_2FC of spliced reads for all genes that have un-spliced reads in each species. Pearson's correlation coefficient (PPC) between the values is shown for each species. **D.** Number of genes with differential nascent proportion (DNP) for each species, which are up- or down-regulated in zygotes. **E, F.** Upset plots of increased/decreased DNP genes and upregulated/downregulated DEGs in mice (E) and rats (F). **G.** Average intronic coverage for *Oog2, Obox2, Obox7, Nlrp4g* and *Zar1* that were called DNP, in

oocytes and zygotes, red boxes highlight regions with intronic coverage. * $p < 0.05$, ** $p<0.01$ and *** $p<0.005$, student's t-test.

Differential splicing might play a role in MZT in both mice and rats

To uncover genes with splicing changes and isoform switches during MZT, we performed DTU analysis (Materials and Methods) on genes between oocytes and zygotes of both species. We found that 2,601 genes exhibited DTU between mouse oocytes and zygotes, while only 609 genes showed DTU between rat oocytes and zygotes (Figure 4A), once more suggests a much more dynamic transcriptional landscape in the mouse zygotes than in rat zygotes. In both species, differential transcript usage can be attributed to the differential expression of no more than two isoforms. (Supplementary Figure 2B). Only small portions of DEGs overlapped genes with DTUs and vice versa in both species (Figure 4B). Interestingly, the number (308) of DTU genes in mice that also are upregulated DEGs is close to the number (324) of DTU genes that also are downregulated DEGs, despite many more downregulated DEGs in this species (Figure 4B). This might suggest that some of the upregulated DEGs might be, at the very least, newly modified transcripts that preside in the cytoplasm of zygotes. DTU genes in mice significantly enriched for GO BP terms such as mitotic cell cycle and protein ubiquitination (Figure 4C), while DTU genes in rats did not significantly enrich for any GO BP terms (FDR < 0.05) (Figure 4D). Albeit top ranked GO BP terms by p-values (without multiple hypotheses test correction) for both mice and rats are related to cell cycle. DTU genes in both species also are involved in histone modification, chromatin organization, protein ubiquitination and modification (Figures 4C, 4D), suggesting a role of alternative splicing in ZGA associated chromatin remodeling. For instance, we found *Bap* and *Usp3* exhibiting DTU in mice (Figures 5A, 5B), and *Usp16* and *Rnf2* showing DTU in rats (Figures 5C, 5D). These results are consistent with previous findings that *Usp3* and *Bap1*

deubiquitinate H2AK119ub1 (Sharma et al., 2014; Thomas et al., 2023), *Usp16* is the dominant deubiquitinase of H2AK119ub1 in oocytes(Rong et al.), while Rnf2 monoubiquitinates H2A histone (Wang et al.). Chromatin undergoes drastic changes during MZT including redistribution of histone H2A among other epigenetic makers, and thus, the control of H2A is vital to ensure proper embryonic development (Wu et al.). Previous studies have shown that both accumulation and absence of H2A may result in embryonic arrest(Chen et al., 2021; Rong et al., 2022). Furthermore, we found that some genes with DTU (such as *Usp*16) did not exhibit overall expression level changes in both mice and rats. Thus, the switches in isoform usage may originate from both newly transcribed and degraded transcripts and may play roles in MZT in both mice and rats.

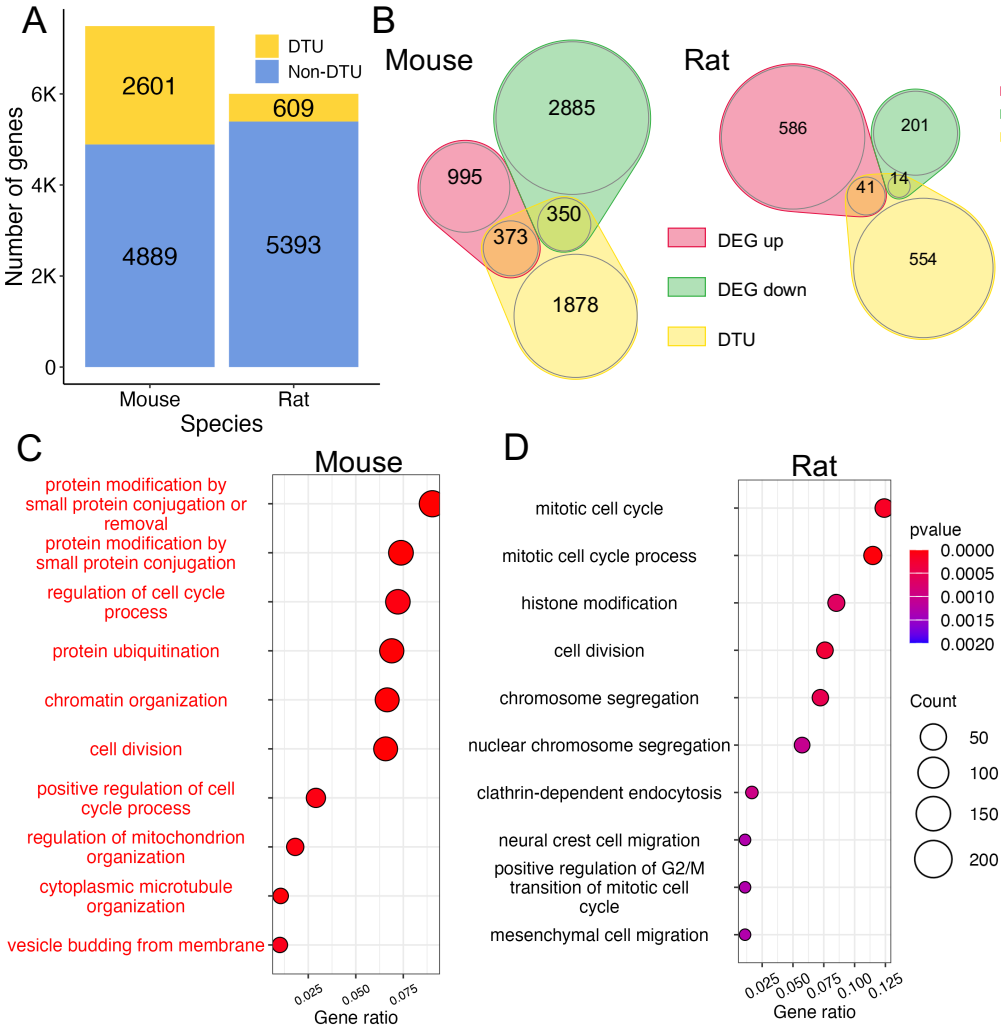

Figure 4. Differential splicing of transcripts between oocytes and zygotes of mice and rats. A. Number of transcribed genes with and without DTU (FDR < 0.05) in each species. **C.** Venn diagram of DTU genes and upregulated or downregulated DEGs in each species. **D.** GO BP term enrichment for mouse genes with DTU (top 10 terms are shown, names marked in red are significant (FDR < 0.05). **E.** Go BP term enrichment for rat genes with DTU (top 10 terms are shown). Gene ratio is the ratio of genes in a GO BP term that were called DTU over all genes in that term.

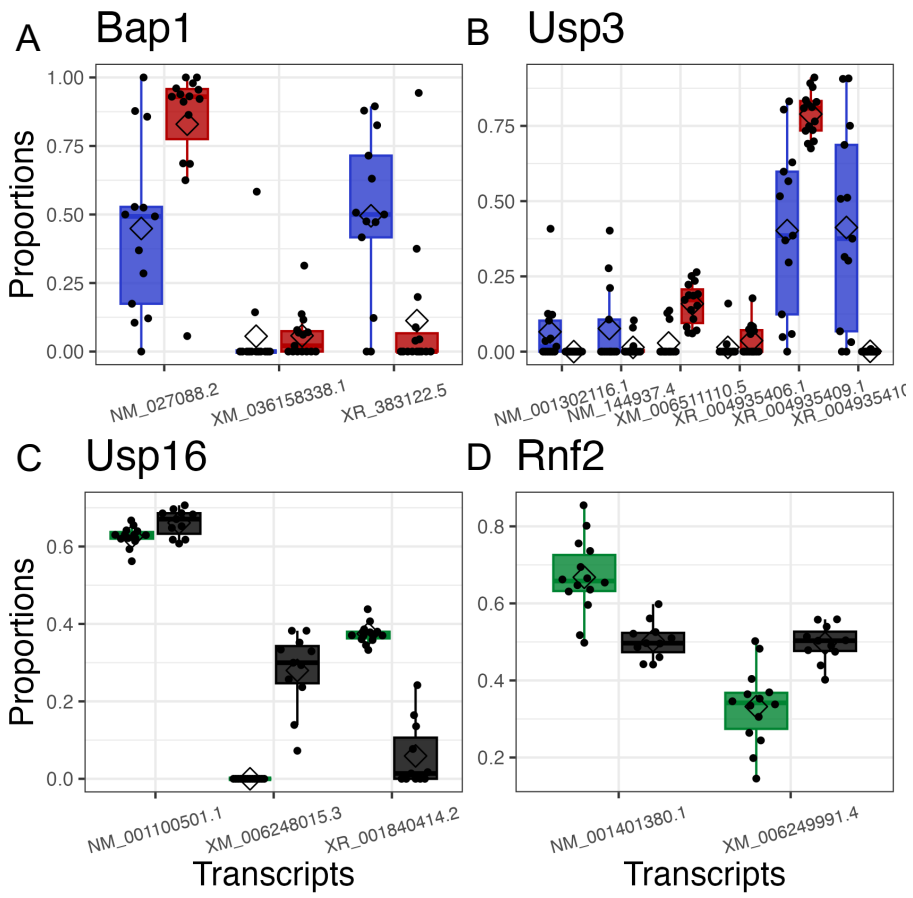

Figure 5. A-D Comparison of proportions of isoforms of *Bap1*(**A**)*, Usp3* (**B**), *Usp16* (**C**) and *Rnf2* (**D**) between oocytes and zygotes of mice and rats.

Genes transcripts in oocytes and zygotes undergo distinct 3'UTR polyadenylations in both mice and rats

Post-transcriptional modifications to mRNA molecules such as alternative use of polyadenylation sites in 3'UTRs, play a critical role in the regulation of mRNA stability and translation (Mayya & Duchaine, 2019; Mignone et al., 2002). Thus, we analyzed differences in 3'UTR usage of transcribed genes between oocytes and zygotes in both species by calculating a PDUI (Percentage of Distal poly-A site Usage Index) value (Feng et al., 2018; Xia et al., 2014) for each expressed gene (Materials and Methods). Oocytes and zygotes in each species could be clearly differentiated based on their PDUI values in UMAP displays (Figures 6A, 6B), indicating that genes expressed

in oocytes and zygotes underwent distinct 3'UTR polyadenylations. We then sought to uncover significant differences in 3'UTR usage between oocytes and zygotes (Materials and Methods). In mice, we found that 1020 genes exhibited significantly differential alternative polyadenylation (DAP) between oocytes and zygotes; of which, 785 (76.9%) showed increases in proximal adenylation site usage (preference for shorter 3'UTRs), while the remaining 186 (23.0%) showed preference for distal polyadenylation (preference for longer 3'UTRs) (Figure 6C). In rats, we found that 154 genes showed significant DAP between oocytes and zygotes; of which, 106 (55.2%) had increased preference for distal adenylation sites, while the remaining 86 (44.8%) showed increased preference for proximal sites (Figure 6C). Thus, the much greater proportion of genes with shortened 3'UTRs in mouse zygotes than in rat zygotes suggests that mouse zygotes undergo much more extensive de-polyadenylation modifications than rat zygotes.

We then investigated the relationships between DEGs and DAP genes. In mice, a considerable number of DAP genes were also DEGs. Specifically, of the mouse DAP genes with shortened 3'UTRs, 288 were upregulated DEGs, but only 35 were downregulated DEG, even though there were fewer upregulated DEGs than downregulated DEGs (Figure 1C). Of the mouse DAP genes with lengthened 3'UTRs, 14 were upregulated DEGs, and 37 was downregulated DEGs (Figure 6D). These results indicate that DAP genes in mice with shortened 3'UTRs tend to be upregulated DEGs(Figure 6D). In addition, we analyzed the Log2FC changes of all genes analyzed for DAP (Figure 6E) and found that though genes with shortened 3'UTRs tended to be upregulated (skewed towards Log2FC > 0), there was no correlation between the magnitude of expression change and change of 3'UTR usage (PDUI difference). We also add that significant DAP genes with lengthened 3'UTRs showed no apparent association with upregulation/downregulation, and that downregulated genes also did not show apparent

association with lengthened/shortened 3'UTRs. In rats, only a few DAP genes were also DEGs, with no correlation between the numbers of DEGs and DAPs (Supplementary Figure 3A), thus no confident conclusion could be drawn. DAP genes with shortened 3'UTRs in mice are enriched for mitotic cell cycle transition as well as meiotic division (Figure 6F). Although no GO terms are significantly enriched for the DAP genes after false discovery rate correction (FDR < 0.05), top ranked (by p-value) GO terms enriched by significant DAP genes in rats include protein ubiquitination, positive regulation of miRNA mediated gene silencing and positive regulation of G2/M transition of mitotic cell (Supplementary Figure 3B).

Many of DAP genes in mice or rats have been known to play various roles in the MZT. We describe two sets of such genes below. The first set are involved in deadenylation and readenylation of mRNAs. We found that *Btg4* and *Cnot7* had DAP with shortened 3'UTRs in mice (Figure 6G). It has been shown that CNOT7 along with CNOT6/6l/8 form the CCR4-NOT complex that controls deadenylation of mRNAs (Aslam et al., 2009; Horvat et al., 2018; Ma et al., 2015; Sha et al., 2018). It is recently reported that BTG4 functions as a mediator of deadenylation, playing a critical role in the production of substrates for maternal RNA re-adenylation during MZT in humans(Liu et al., 2016; Pasternak et al., 2016; Sha et al., 2020). It is likely that these deadenylation related genes switch their transcription modes in zygotes to produce transcripts with shorter 3'UTRs via deadenylation followed by re-adenylation, thereby conferring higher translational efficiency of the genes.

The second set of genes are implicated in the regulation of mitotic progression and cell cycle. We found that *Nek7* had DAP with shortened 3'UTR in mouse zygotes (Figure 6G). An early study has shown that reduction in *Nek7* activity can cause cells to arrest in metaphase of mitosis (Salem et al., 2010). It is likely that *Nek7* serves a similar function in meiosis through an

inhibitory mechanism due to a longer 3'UTR in MII oocytes. Interestingly, unlike the case in mice, several mitosis related DAP genes in rats exhibited lengthened 3'UTR usage. The *Mastl* gene, which encodes an essential regulator of cell cycle control (Rogers et al., 2018), exhibited increased usage of longer 3'UTR transcripts in rat zygotes (Figure 6H). Similarly, *Cdc25a* encoding a protein phosphatase that functions as a critical cell cycle regulator (Shen & Huang, 2012), exhibited increased usage of longer 3'UTRs (Figure 6H). These results suggest different regulatory mechanisms of mRNA stability and protein translation in rat and mouse zygotes during the first mitotic progression.

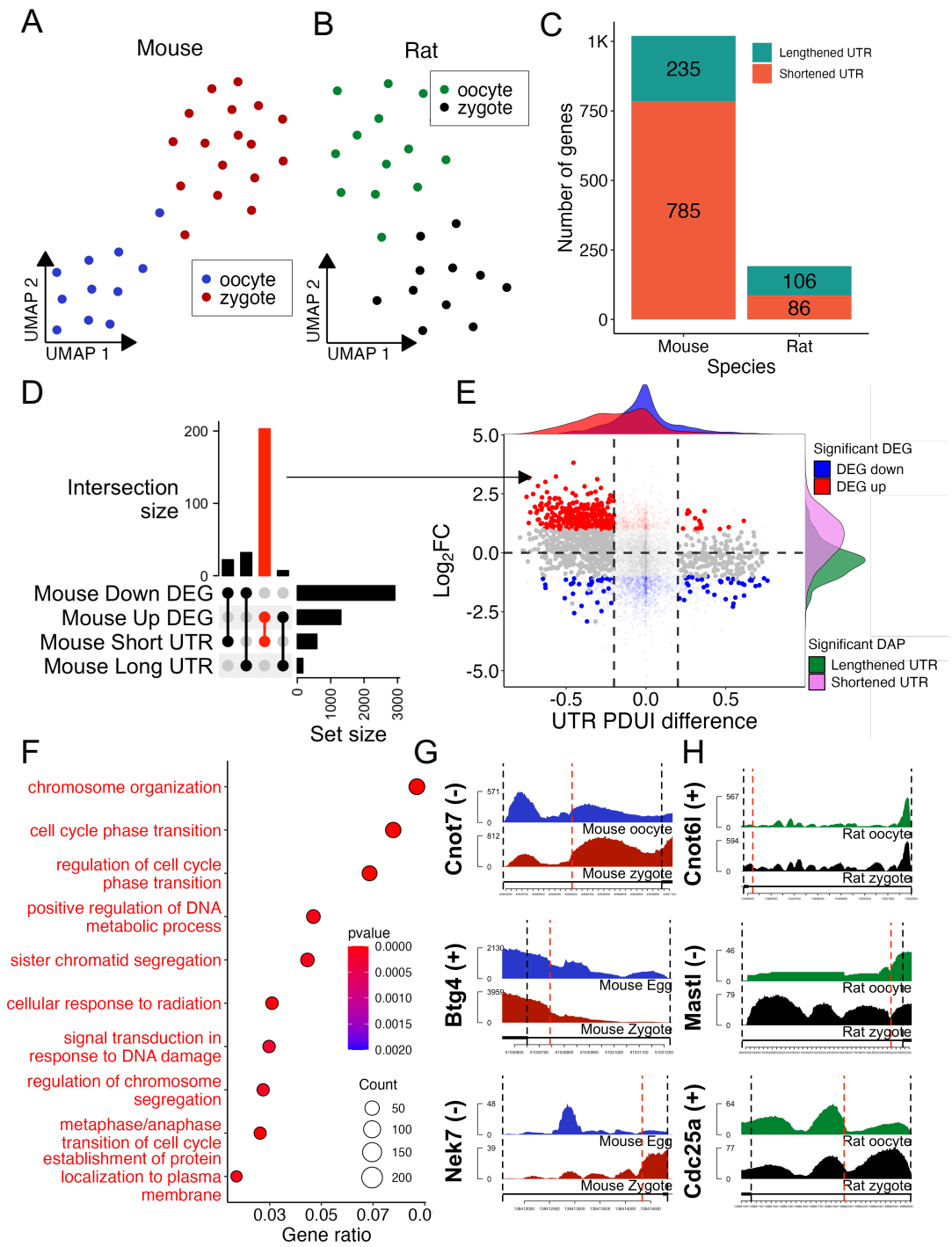

Figure 6. Differential alternative polyadenylation of transcripts between oocytes and zygotes of mice and rats. A,B UMAP display of mouse (A) and rat (B) oocytes and zygotes based on PDUI values of genes. **C**. Number of genes with lengthened and shortened UTRs in zygotes relative to in oocytes of mice and rats. **D.** Upset plot of DAP genes and DEGs in mice. E. Log_2FC expression vs PDUI difference for all genes that were analyzed for DAP; low transparency points are genes not significant for DAP, red/blue genes are significantly up/down regulated respectively; pink and green density plots show Log2FC distribution for significant DAP genes with lengthened and shortened UTRs; red and blue density plots show PDUI changes for significantly up/down

regulated DEGs. **F.** Significantly enriched GO BP terms for DAP genes in mice (FDR < 0.05). **G.** Reads coverage on the 3'UTRs of mouse genes *Cnot7, Btg4* and *Nek7*. **H.** Read coverage on the 3'UTRs of rat genes *Cnot6l, Mastl* and *Cdc25a.* In both H) and I), red lines mark the predicted proximal polyadenylation sites.

Most of orthologous genes in mice and rats have similar while a small portion have opposite transcriptional patterns.

We sought to investigate to what extent DEG, DNP, DTU and DAP genes in mice and rats are conserved based on their orthologous relations. Surprisingly, even though the two species share many orthologous genes (21,824 genes), of which only about 4% (889) were found to be significantly differentially expressed (FDR < 0.05, $|\log_2 FC| > \log_2 1.25$) in zygotes relative to in oocytes in both species. However, most (627, or 70.5%) of the orthologous DEGs showed similar tendency of change (257 upregulated and 370 downregulated) (Figure 7A), while the rest small portion (262 or 29.5%) exhibited opposite changes, i.e., 74 upregulated DEGs in mice were downregulated DEGs in rats, and 188 downregulated DEGs in mice were upregulated DEGs in rats (Figure 7A). These results suggest that most of the orthologous genes that exhibit changes in both species behave similarly in terms of transcriptional change. These orthologous DEGs are enriched for multiple GO BPs that might be crucial to MZT in the two species (Figures 7B, 7C). Orthologous DEGs that were generally upregulated in both species were enriched for transport of transcripts and the cell cycle, while DEGs that were downregulated in both species were enriched for cytoplasmic translation and Nonsense-mediated decay. Orthologous DEGs that were upregulated in rats but downregulated in mice were enriched for the TCA cycle, RNA splicing and rRNA processing (Figures 7B and 7C).

There are only seven orthologous genes with DNPs in both mice and rats (Supplementary Figure 4A). Nonetheless, some may play essential roles in MZT. For instance, the *Oog1* gene

encoding oogenesin exhibited increased nascent proportions in both mouse and rat zygotes (Figure 7D). It has been shown that oogenesin plays critical roles in zygotic transcription (Minami et al., 2003). Moreover, *Nlrp4b* showed decreased nascent proportion in both mouse and rat zygotes (Figure 7D). Studies have shown that *Nlrp4a-g* may play important roles in early pre-implantation embryos, with high expression of NLRP4G and NLRP4E in both oocytes and zygotes (Chang et al., 2013; Li et al., 2015).

There were 210 orthologous genes with DTU in both mice and rats (Supplementary Figure 4B), they were enriched for positive regulation of transcription elongation by RNA polymerase II (FDR < 0.05). Finally, a total of 53 orthologous genes had DAP in both species, with either lengthened or shortened 3'UTR in both species mostly aligned (Figure 7E). Close inspection finds many interesting orthologous DAP genes. For instance, *Eif4e* (Figure 7F) encoding a rate-limiting regulator of translation of (Duncan et al., 1987; Hiremath et al., 1985), exhibited preference for shortened 3'UTR in both rat and mouse zygotes (Figure 7F), implying higher translational efficiency of the transcripts to prepare the zygotes for higher levels of protein production in the later stages. It has also been shown that Eif4e interacts with CNOT7 via BTG4, thereby expediting maternal mRNA degradation during MZT (Liu et al., 2016; Pasternak et al., 2016). Moreover, both *Usp28* and *Bmi1* exhibited shortened 3'UTRs in both mouse and rat zygotes (Figure 7F). Though the products of both genes participate in the regulation of histone H2A, it has been shown that Usp28 is a deubiquitinase of H2A(Li et al., 2019), while Bmi1 forms the core protein of the Polycomb Repressive Complex 1 (PRC1), which mono-ubiquitinates H2A histones (Abdouh et al., 2016). This result, along with the DTU changes mentioned prior, suggests a role of post-transcriptional splicing and polyadenylation regulating chromatin states for ZGA in both species. In addition, both *Anapc1* and *Arid1a* exhibited lengthened 3'UTRs in both mouse and rat zygotes

(Figure 7F). *Anapc1* encodes a subunit of the Anaphase Promoting Complex/Cyclosome (APC/C), a key ubiquitin-ligase in mitosis. It has recently been shown that delay in the APC/C activation extends mitosis in mouse embryos (Ajeawung et al., 2019). Thus, our results may provide a putative regulatory mechanism of *Anapc1* via 3'UTR extension, which may in turn limit translational efficiency and cause delays in subsequent mitosis (Ajduk et al., 2017). *Arid1a* encodes a subunit of chromatin remodeling complexes, and its expression in mouse embryos has been found to accumulate during G0 phase and vanish by mitosis (Flores-Alcantar et al., 2011). The lengthened 3'UTR of *Arid1a* transcripts in both mouse and rat zygotes may represent a snapshot in the first cell cycle of the embryo, implying a post-transcriptional regulating mechanism through extension of 3'UTR tails (Flores-Alcantar et al., 2011).

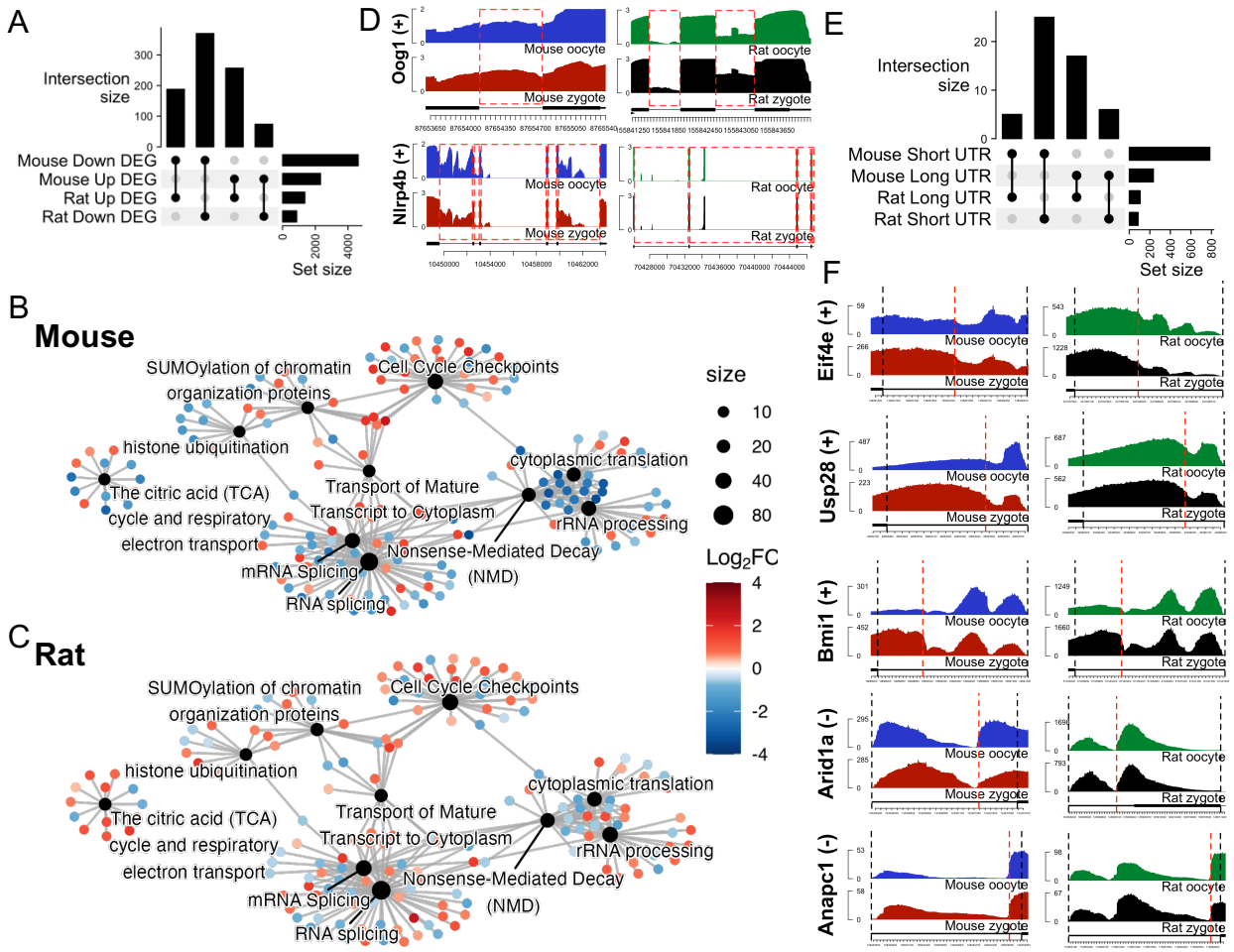

Figure 7. Orthologous genes in mice and rats may have similar or opposite transcriptional patterns. A. Upset plot of upregulated and downregulated orthologous DEGs in zygotes relative to oocytes of mice and rats. **B, C.** Enriched GO BP terms for orthologous DEGs in mice (B) and rats (C). **D.** Read coverages of orthologous DNP genes *Oog1* and *Nlrp4b* in oocytes and zygotes of mice and rats. **E.** Upset plot of orthologous DAP genes in mice and rats. **F. 3'**UTR expression of orthologous DAP genes *Eif4e, Usp28, Bmi1, Arid1a,* and *Anapc1* in mice and rats.

Discussion

Our analysis of DEGs between oocytes and zygotes of mice and rats revealed new different facets of the underlying workings of their early MZT. Most prominently, we found decreases in ribosomal protein and nonsense-mediated mRNA decay related transcripts in zygotes of both species, though to a lesser degree in rats. We also found significant increases in transcripts of genes related to the cell cycle, mRNA transport and transcription initiation in mouse zygotes. Although most transcripts in mouse zygotes undergo degradation upon fertilization, there are clearly newly produced transcripts. Moreover, the increased transcripts of nucleoporin genes in mouse zygotes suggest increased transport of transcripts into the cytoplasm from the nucleus, which could also explain observed upregulation of many genes even in the absence of true transcription. On the other hand, upregulated genes in rat zygotes are enriched for the TCA cycle, hinting at a requirement for more energy production after fertilization. Conversely, the TCA cycle genes involved in energy production were downregulated in mice, while the genes involved in acetyl-CoA synthesis from pyruvate were upregulated. These results could be due to differences in the timing of events, whereby the mouse zygote prepares its first mitosis earlier and in a more active manner, while the rat zygote has still yet begun degradation of maternal transcripts. However, our detection of numerous upregulated genes in zygotes relative to oocytes in rats, suggesting that MZT might occur in rat zygotes, though at a smaller scale than in mouse zygotes.

Our analysis on intronic transcripts of genes found overall increases in the proportion of intronic reads and number of genes with intronic transcripts in both species after fertilization, indicating an increase of nascent transcription in zygotes. This was particularly true in mice, despite the majority of DEGs found to be downregulated. Previous studies have suggested that the increases in nascent transcription in the zygote is in part due to promiscuous transcription of genes

and inefficient splicing during minor zygotic activation in mice(Abe et al., 2015), and our results suggest that a similar process might occur in the rat zygotes as well. In addition, coupled with the increased expression activity related to RNA transport, particularly in mice, these changes in nascent and mature transcript proportions may also at least partially result from increased RNA transport from the nucleus to the cytosol.

The observed changes in isoform usage between oocytes and zygotes of both species indicate post-transcriptional regulation of genes in zygotes. Interestingly, cell cycle was a top enriched process for genes with differential transcript usage in both mice and rats. It is worth noting that several genes that regulate histone H2A show strong differential isoform usage and differential poly-adenylation in both mice and rats. These results advocate for similar epigenetic regulations of chromatins in both species by differential isoform usage. Though more details remain to be revealed, our results suggest similar post-transcriptional events in zygotes of mice and rats.

Our analysis of differential polyadenylation reveals that transcripts undergo distinct 3'UTR polyadenylations in oocytes and zygotes of both species. We would be remiss to not touch on the issue of differences in gene-body read distribution between oocytes and zygotes and the subsequent impact on alternative polyadenylation analysis. The stronger 3'-end bias of reads in mouse oocytes than in mouse zygotes is unlikely due to technical factors but rather biological differences between mouse oocytes and zygotes, which is not the case in rat oocytes and rat zygotes. Such bias in mouse samples should be negligible on our DAP analysis, since similar 3'UTR preference of the same gene would result in similar bias observed in read coverage (exhibiting similar peaks in the 3'UTR region), while only differences in 3'UTR length preference (caused by differential poly-A cleavage sites) would result in peaks appearing in one group and not in the other. Another issue that has been brought up in previous studies regarding transcriptomic profiles

of 1-cell stage zygotes obtained via poly-A enrichment techniques is inflation of expression values due to inherent biases towards longer Poly-A tails in poly-A capture RNA-seq methodologies (Viscardi & Arribere). Previous studies have also held conflicting views towards the length of poly-A tails in zygotic transcripts. For example, one study (Lee et al., 2024) reported extensive shortening of poly-A tails in the zygote, while another (Liu et al., 2021) suggested a shift towards longer poly-A tail lengths from MII oocytes to zygotes. Though we were not able to quantify for poly-A tail length in our study, we found an overwhelmingly larger overlap between shortened 3'UTRs and upregulated genes in mouse zygotes, compared to other overlaps between DAP and DEG genes. Yet, we note that there is no correlation between the changes in expression levels and the changes in 3'UTR preference measured by PDUI. Taken together, it is unclear whether the observed upregulation is indirectly caused by changes in poly-adenylation, and it appears that many other genes do not experience significant changes in polyadenylation but are upregulated regardless in mouse zygotes. The case in rats is even more prominent, with most upregulated genes experiencing no significant change in 3'UTR preference.

Although most orthologous genes in mice and rats had similar differential transcriptional patterns in term of DGEs, DNT, DTU and DAP during MZT, others showed different patterns. In summary, these orthogonal analyses on the transcriptomic changes during the oocyte to zygote transition in mice and rats strongly suggest minor zygotic activation is a vibrant process in both species, albeit a delayed and weaker process in rats. Much of the observed results also confirm significant post-transcriptional regulation, most notably in the form of alternative polyadenylation, in both species.

Future studies should involve a multi-omics approach for both species, with strong emphasis on post-transcriptional modifications such as poly-adenylation and epigenetic

regulations of expression. Furthermore, the lack of transcript degradation in rat zygotes may imply that timing of rat zygotes and mouse zygotes differ in the progression of MZT. However, there was a much greater number of upregulated DEGs observed in the rat, perhaps owing to transient expressions of the maternal genome upon fertilization. Thus, a more comprehensive analysis could focus on finer-grained snapshots of the zygote in both mice and rats to capture transient expressions of genes, as well as timing of minor zygotic activation.

References

Abdouh, M., Hanna, R., El Hajjar, J., Flamier, A., & Bernier, G. (2016). The Polycomb Repressive Complex 1 Protein BMI1 Is Required for Constitutive Heterochromatin Formation and Silencing in Mammalian Somatic Cells. *Journal of Biological Chemistry*, *291*(1), 182-197. https://doi.org/10.1074/jbc.m115.662403

Abe, K. I., Funaya, S., Tsukioka, D., Kawamura, M., Suzuki, Y., Suzuki, M. G., Schultz, R. M., & Aoki, F. (2018). Minor zygotic gene activation is essential for mouse preimplantation development. *Proc Natl Acad Sci U S A*, *115*(29), E6780-E6788. https://doi.org/10.1073/pnas.1804309115

Abe, K. I., Yamamoto, R., Franke, V., Cao, M., Suzuki, Y., Suzuki, M. G., Vlahovicek, K., Svoboda, P., Schultz, R. M., & Aoki, F. (2015). The first murine zygotic transcription is promiscuous and uncoupled from splicing and 3′ processing. *The EMBO Journal*, *34*(11), 1523-1537. https://doi.org/10.15252/embj.201490648

Ajduk, A., Strauss, B., Pines, J., & Zernicka-Goetz, M. (2017). Delayed APC/C activation extends the first mitosis of mouse embryos. *Scientific Reports*, *7*(1), 9682. https://doi.org/10.1038/s41598-017-09526-1

Ajeawung, N. F., Nguyen, T. T. M., Lu, L., Kucharski, T. J., Rousseau, J., Molidperee, S., Atienza, J., Gamache, I., Jin, W., Plon, S. E., Lee, B. H., Teodoro, J. G., Wang, L. L., & Campeau, P. M. (2019). Mutations in ANAPC1, Encoding a Scaffold Subunit of the Anaphase-Promoting Complex, Cause Rothmund-Thomson Syndrome Type 1. *The American Journal of Human Genetics*, *105*(3), 625-630. https://doi.org/10.1016/j.ajhg.2019.06.011

Anders, S., Pyl, P. T., & Huber, W. (2015). HTSeq--a Python framework to work with high-throughput sequencing data. *Bioinformatics*, *31*(2), 166-169. https://doi.org/10.1093/bioinformatics/btu638

Anders, S., Reyes, A., & Huber, W. (2012). Detecting differential usage of exons from RNA-seq data. *Genome Research*, *22*(10), 2008-2017. https://doi.org/10.1101/gr.133744.111

Aoki, F., Worrad, D. M., & Schultz, R. M. (1997). Regulation of transcriptional activity during the first and second cell cycles in the preimplantation mouse embryo. *Dev Biol*, *181*(2), 296-307. https://doi.org/10.1006/dbio.1996.8466

Aslam, A., Mittal, S., Koch, F., Andrau, J.-C., & Winkler, G. S. (2009). The Ccr4–Not Deadenylase Subunits CNOT7 and CNOT8 Have Overlapping Roles and Modulate Cell Proliferation. *Molecular Biology of the Cell*, *20*(17), 3840-3850. https://doi.org/10.1091/mbc.e09-02-0146

Berg, J. M., Tymoczko, J. L., & Stryer, L. (2002). *Biochemistry, Fifth Edition*. W.H. Freeman. https://books.google.com/books?id=uDFqAAAAMAAJ

Blake, J. A., Baldarelli, R., Kadin, J. A., Richardson, J. E., Smith, L., Cynthia, Bult, C. J., Anagnostopoulos, A. V., Beal, J. S., Bello, S. M., Blodgett, O., Butler, N. E., Campbell, J., Christie, K. R., Corbani, L. E., Dolan, M. E., Drabkin, H. J., Flores, M., Giannatto, S. L., Guerra, A., . . . Zhu, Y. S. (2021). Mouse Genome Database (MGD): Knowledgebase for mouse–human comparative biology. *Nucleic Acids Research*, *49*(D1), D981-D987. https://doi.org/10.1093/nar/gkaa1083

Bray, N. L., Pimentel, H., Melsted, P., & Pachter, L. S. (2015). Near-optimal RNA-Seq quantification. *ArXiv*, *abs/1505.02710*.

Chang, B.-H., Liu, X., Liu, J., Quan, F.-S., Guo, Z.-K., & Zhang, Y. (2013). Developmental expression and possible functional roles of mouse Nlrp4e in preimplantation embryos. *In*

Vitro Cellular & Developmental Biology - Animal, *49*(7), 548-553. https://doi.org/10.1007/s11626-013-9638-9

Chen, Z., Djekidel, M. N., & Zhang, Y. (2021). Distinct dynamics and functions of H2AK119ub1 and H3K27me3 in mouse preimplantation embryos. *Nature Genetics*, *53*(4), 551-563. https://doi.org/10.1038/s41588-021-00821-2

Ciccarone, F., Vegliante, R., Di Leo, L., & Ciriolo, M. R. (2017). The TCA cycle as a bridge between oncometabolism and DNA transactions in cancer. *Seminars in Cancer Biology*, *47*, 50-56. https://doi.org/10.1016/j.semcancer.2017.06.008

Cler, E., Papai, G., Schultz, P., & Davidson, I. (2009). Recent advances in understanding the structure and function of general transcription factor TFIID. *Cellular and Molecular Life Sciences*, *66*(13), 2123-2134. https://doi.org/10.1007/s00018-009-0009-3

Duncan, R., Milburn, S. C., & Hershey, J. W. (1987). Regulated phosphorylation and low abundance of HeLa cell initiation factor eIF-4F suggest a role in translational control. Heat shock effects on eIF-4F. *J Biol Chem*, *262*(1), 380-388.

Eichhorn, S. W., Subtelny, A. O., Kronja, I., Kwasnieski, J. C., Orr-Weaver, T. L., & Bartel, D. P. (2016). mRNA poly(A)-tail changes specified by deadenylation broadly reshape translation in Drosophila oocytes and early embryos. *Elife*, *5*. https://doi.org/10.7554/eLife.16955

Feng, X., Li, L., Wagner, E. J., & Li, W. (2018). TC3A: The Cancer 3′ UTR Atlas. *Nucleic Acids Research*, *46*(D1), D1027-D1030. https://doi.org/10.1093/nar/gkx892

Finak, G., McDavid, A., Yajima, M., Deng, J., Gersuk, V., Shalek, A. K., Slichter, C. K., Miller, H. W., McElrath, M. J., Prlic, M., Linsley, P. S., & Gottardo, R. (2015). MAST: a flexible statistical framework for assessing transcriptional changes and characterizing heterogeneity in single-cell RNA sequencing data. *Genome Biol*, *16*, 278. https://doi.org/10.1186/s13059-015-0844-5

Flores-Alcantar, A., Gonzalez-Sandoval, A., Escalante-Alcalde, D., & Lomelí, H. (2011). Dynamics of expression of ARID1A and ARID1B subunits in mouse embryos and in cells during the cell cycle. *Cell and Tissue Research*, *345*(1), 137-148. https://doi.org/10.1007/s00441-011-1182-x

Gene Ontology, C. (2021). The Gene Ontology resource: enriching a GOld mine. *Nucleic Acids Res*, *49*(D1), D325-D334. https://doi.org/10.1093/nar/gkaa1113

Guo, C., Kong, F., Lv, Y., Gao, N., Xiu, X., & Sun, X. (2020). CDC20 inhibitor Apcin inhibits embryo implantation in vivo and in vitro. *Cell Biochemistry and Function*, *38*(6), 810-816. https://doi.org/10.1002/cbf.3550

Guo, Q., Liu, Q., Wang, N., Wang, J., Sun, A., Qiao, J., & Yan, L. (2022). The function of Nucleoporin 37 on mouse oocyte maturation and preimplantation embryo development. *Journal of Assisted Reproduction and Genetics*, *39*(1), 107-116. https://doi.org/10.1007/s10815-021-02330-x

Hiremath, L. S., Webb, N. R., & Rhoads, R. E. (1985). Immunological detection of the messenger RNA cap-binding protein. *J Biol Chem*, *260*(13), 7843-7849.

Horvat, F., Fulka, H., Jankele, R., Malik, R., Jun, M., Solcova, K., Sedlacek, R., Vlahovicek, K., Schultz, R. M., & Svoboda, P. (2018). Role of *Cnot6l* in maternal mRNA turnover. *Life Science Alliance*, *1*(4), e201800084. https://doi.org/10.26508/lsa.201800084

Ji, S., Chen, F., Stein, P., Wang, J., Zhou, Z., Wang, L., Zhao, Q., Lin, Z., Liu, B., Xu, K., Lai, F., Xiong, Z., Hu, X., Kong, T., Kong, F., Huang, B., Wang, Q., Xu, Q., Fan, Q., . . . Xie, W.

(2023). OBOX regulates mouse zygotic genome activation and early development. *Nature*, *620*(7976), 1047-1053. https://doi.org/10.1038/s41586-023-06428-3

Juven-Gershon, T., Hsu, J.-Y., Theisen, J. W., & Kadonaga, J. T. (2008). The RNA polymerase II core promoter — the gateway to transcription. *Current Opinion in Cell Biology*, *20*(3), 253-259. https://doi.org/10.1016/j.ceb.2008.03.003

Kafkia, E., Andres-Pons, A., Ganter, K., Seiler, M., Smith, T. S., Andrejeva, A., Jouhten, P., Pereira, F., Franco, C., Kuroshchenkova, A., Leone, S., Sawarkar, R., Boston, R., Thaventhiran, J., Zaugg, J. B., Lilley, K. S., Lancrin, C., Beck, M., & Patil, K. R. (2022). Operation of a TCA cycle subnetwork in the mammalian nucleus. *Science Advances*, *8*(35). https://doi.org/10.1126/sciadv.abq5206

Kanehisa, M., Furumichi, M., Sato, Y., Kawashima, M., & Ishiguro-Watanabe, M. (2022). KEGG for taxonomy-based analysis of pathways and genomes. *Nucleic Acids Res*. https://doi.org/10.1093/nar/gkac963

Kanehisa, M., & Goto, S. (2000). KEGG: kyoto encyclopedia of genes and genomes. *Nucleic Acids Res*, *28*(1), 27-30. https://doi.org/10.1093/nar/28.1.27

Kim, D., Paggi, J. M., Park, C., Bennett, C., & Salzberg, S. L. (2019). Graph-based genome alignment and genotyping with HISAT2 and HISAT-genotype. *Nat Biotechnol*, *37*(8), 907-915. https://doi.org/10.1038/s41587-019-0201-4

Krueger, F. (2015). Trim galore. *A wrapper tool around Cutadapt and FastQC to consistently apply quality and adapter trimming to FastQ files*, *516*, 517.

Lee, K., Cho, K., Morey, R., & Cook-Andersen, H. (2024). An extended wave of global mRNA deadenylation sets up a switch in translation regulation across the mammalian oocyte-to-embryo transition. *Cell Reports*, *43*(2), 113710. https://doi.org/10.1016/j.celrep.2024.113710

Lee, M. T., Bonneau, A. R., & Giraldez, A. J. (2014). Zygotic genome activation during the maternal-to-zygotic transition. *Annu Rev Cell Dev Biol*, *30*, 581-613. https://doi.org/10.1146/annurev-cellbio-100913-013027

Li, F., Han, H., Sun, Q., Liu, K., Lin, N., Xu, C., Zhao, Z., & Zhao, W. (2019). USP28 regulates deubiquitination of histone H2A and cell proliferation. *Exp Cell Res*, *379*(1), 11-18. https://doi.org/10.1016/j.yexcr.2019.03.026

Li, H., Handsaker, B., Wysoker, A., Fennell, T., Ruan, J., Homer, N., Marth, G., Abecasis, G., & Durbin, R. (2009). The Sequence Alignment/Map format and SAMtools. *Bioinformatics*, *25*(16), 2078-2079. https://doi.org/10.1093/bioinformatics/btp352

Li, W., Lin, X., Peng, H., & Zhang, W. (2015). Expression and localization of Nlrp4g in mouse preimplantation embryo. *Zygote*, *23*(6), 846-851. https://doi.org/10.1017/S0967199414000525

Liu, Y., Lu, X., Shi, J., Yu, X., Zhang, X., Zhu, K., Yi, Z., Duan, E., & Li, L. (2016). BTG4 is a key regulator for maternal mRNA clearance during mouse early embryogenesis. *Journal of Molecular Cell Biology*, *8*(4), 366-368. https://doi.org/10.1093/jmcb/mjw023

Liu, Y., Nie, H., Zhang, C., Hou, Z., Wang, J., & Lu, F. (2021). *Poly(A) tail length is a major regulator of maternal gene expression during the mammalian oocyte-to-embryo transition*. Cold Spring Harbor Laboratory.

Liu, Y., Zhao, H., Shao, F., Zhang, Y., Nie, H., Zhang, J., Li, C., Hou, Z., Chen, Z.-J., Wang, J., Zhou, B., Wu, K., & Lu, F. (2023). Remodeling of maternal mRNA through poly(A) tail orchestrates human oocyte-to-embryo transition. *Nature Structural & Molecular Biology*, *30*(2), 200-215. https://doi.org/10.1038/s41594-022-00908-2

Love, M. I., Huber, W., & Anders, S. (2014). Moderated estimation of fold change and dispersion for RNA-seq data with DESeq2. *Genome Biology*, *15*(12). https://doi.org/10.1186/s13059-014-0550-8

Love, M. I., Soneson, C., & Patro, R. (2018). Swimming downstream: statistical analysis of differential transcript usage following Salmon quantification. *F1000Research*, *7*, 952. https://doi.org/10.12688/f1000research.15398.3

Ma, J., Flemr, M., Strnad, H., Svoboda, P., & Schultz, R. M. (2013). Maternally recruited DCP1A and DCP2 contribute to messenger RNA degradation during oocyte maturation and genome activation in mouse. *Biol Reprod*, *88*(1), 11. https://doi.org/10.1095/biolreprod.112.105312

Ma, J., Fukuda, Y., & Schultz, R. M. (2015). Mobilization of Dormant Cnot7 mRNA Promotes Deadenylation of Maternal Transcripts During Mouse Oocyte Maturation1. *Biology of Reproduction*, *93*(2), 48-48. https://doi.org/10.1095/biolreprod.115.130344

Martens, M., Ammar, A., Riutta, A., Waagmeester, A., Slenter, D. N., Hanspers, K., R, A. M., Digles, D., Lopes, E. N., Ehrhart, F., Dupuis, L. J., Winckers, L. A., Coort, S. L., Willighagen, E. L., Evelo, C. T., Pico, A. R., & Kutmon, M. (2021). WikiPathways: connecting communities. *Nucleic Acids Res*, *49*(D1), D613-D621. https://doi.org/10.1093/nar/gkaa1024

Mayya, V. K., & Duchaine, T. F. (2019). Ciphers and Executioners: How 3'-Untranslated Regions Determine the Fate of Messenger RNAs. *Front Genet*, *10*, 6. https://doi.org/10.3389/fgene.2019.00006

McGrath, J., & Solter, D. (1984). Completion of mouse embryogenesis requires both the maternal and paternal genomes. *Cell*, *37*(1), 179-183. https://doi.org/10.1016/0092-8674(84)90313-1

Melsted, P., Booeshaghi, A. S., Gao, F., Beltrame, E., Lu, L., Hjorleifsson, K. E., Gehring, J., & Pachter, L. (2019). *Modular and efficient pre-processing of single-cell RNA-seq*. Cold Spring Harbor Laboratory.

Melsted, P., Ntranos, V., & Pachter, L. (2019). The barcode, UMI, set format and BUStools. *Bioinformatics*, *35*(21), 4472-4473. https://doi.org/10.1093/bioinformatics/btz279

Mignone, F., Gissi, C., Liuni, S., & Pesole, G. (2002). *Genome Biology*, *3*(3), reviews0004.0001. https://doi.org/10.1186/gb-2002-3-3-reviews0004

Milacic, M., Beavers, D., Conley, P., Gong, C., Gillespie, M., Griss, J., Haw, R., Jassal, B., Matthews, L., May, B., Petryszak, R., Ragueneau, E., Rothfels, K., Sevilla, C., Shamovsky, V., Stephan, R., Tiwari, K., Varusai, T., Weiser, J., . . . D'Eustachio, P. (2024). The Reactome Pathway Knowledgebase 2024. *Nucleic Acids Research*, *52*(D1), D672-D678. https://doi.org/10.1093/nar/gkad1025

Minami, N., Aizawa, A., Ihara, R., Miyamoto, M., Ohashi, A., & Imai, H. (2003). Oogenesin is a novel mouse protein expressed in oocytes and early cleavage-stage embryos. *Biol Reprod*, *69*(5), 1736-1742. https://doi.org/10.1095/biolreprod.103.018051

Monti, M., & Redi, C. (2009). Oogenesis specific genes (Nobox, Oct4, Bmp15, Gdf9, Oogenesin1 and Oogenesin2) are differentially expressed during natural and gonadotropin-induced mouse follicular development. *Mol Reprod Dev*, *76*(10), 994-1003. https://doi.org/10.1002/mrd.21059

Mullins, L. J., & Mullins, J. J. (2004). Insights from the rat genome sequence. *Genome Biol*, *5*(5), 221. https://doi.org/10.1186/gb-2004-5-5-221

Nagaraj, R., Sharpley, M. S., Chi, F., Braas, D., Zhou, Y., Kim, R., Clark, A. T., & Banerjee, U. (2017). Nuclear Localization of Mitochondrial TCA Cycle Enzymes as a Critical Step in Mammalian Zygotic Genome Activation. *Cell*, *168*(1-2), 210-223.e211. https://doi.org/10.1016/j.cell.2016.12.026

Nakao, A. (2004). RPG: the Ribosomal Protein Gene database. *Nucleic Acids Research*, *32*(90001), 168D-170. https://doi.org/10.1093/nar/gkh004

Ni, Y., Shen, P., Wang, X., Liu, H., Luo, H., & Han, X. (2022). The roles of IDH1 in tumor metabolism and immunity. *Future Oncology*, *18*(35), 3941-3953. https://doi.org/10.2217/fon-2022-0583

Nowicka, M., & Robinson, M. D. (2016). DRIMSeq: a Dirichlet-multinomial framework for multivariate count outcomes in genomics. *F1000Research*, *5*, 1356. https://doi.org/10.12688/f1000research.8900.2

Ou, J., & Zhu, L. J. (2019). trackViewer: a Bioconductor package for interactive and integrative visualization of multi-omics data. *Nat Methods*, *16*(6), 453-454. https://doi.org/10.1038/s41592-019-0430-y

Pasternak, M., Pfender, S., Santhanam, B., & Schuh, M. (2016). The BTG4 and CAF1 complex prevents the spontaneous activation of eggs by deadenylating maternal mRNAs. *Open Biology*, *6*(9), 160184. https://doi.org/10.1098/rsob.160184

Patro, R., Duggal, G., Love, M. I., Irizarry, R. A., & Kingsford, C. (2017). Salmon provides fast and bias-aware quantification of transcript expression. *Nat Methods*, *14*(4), 417-419. https://doi.org/10.1038/nmeth.4197

Picelli, S., Björklund Å, K., Faridani, O. R., Sagasser, S., Winberg, G., & Sandberg, R. (2013). Smart-seq2 for sensitive full-length transcriptome profiling in single cells. *Nat Methods*, *10*(11), 1096-1098. https://doi.org/10.1038/nmeth.2639

Popken, J., Graf, A., Krebs, S., Blum, H., Schmid, V. J., Strauss, A., Guengoer, T., Zakhartchenko, V., Wolf, E., & Cremer, T. (2015). Remodeling of the Nuclear Envelope and Lamina during Bovine Preimplantation Development and Its Functional Implications. *PLoS One*, *10*(5), e0124619. https://doi.org/10.1371/journal.pone.0124619

Quinlan, A. R., & Hall, I. M. (2010). BEDTools: a flexible suite of utilities for comparing genomic features. *Bioinformatics*, *26*(6), 841-842. https://doi.org/10.1093/bioinformatics/btq033

Roeder, R. G. (1996). The role of general initiation factors in transcription by RNA polymerase II. *Trends Biochem Sci*, *21*(9), 327-335.

Rogers, S., Mccloy, R. A., Parker, B. L., Gallego-Ortega, D., Law, A. M. K., Chin, V. T., Conway, J. R. W., Fey, D., Millar, E. K. A., O'Toole, S., Deng, N., Swarbrick, A., Chastain, P. D., Cesare, A. J., Timpson, P., Caldon, C. E., Croucher, D. R., James, D. E., Watkins, D. N., & Burgess, A. (2018). MASTL overexpression promotes chromosome instability and metastasis in breast cancer. *Oncogene*, *37*(33), 4518-4533. https://doi.org/10.1038/s41388-018-0295-z

Rong, Y., Zhu, Y.-Z., Yu, J.-L., Wu, Y.-W., Ji, S.-Y., Zhou, Y., Jiang, Y., Jin, J., Fan, H.-Y., Shen, L., & Sha, Q.-Q. (2022). USP16-mediated histone H2A lysine-119 deubiquitination during oocyte maturation is a prerequisite for zygotic genome activation. *Nucleic Acids Research*, *50*(10), 5599-5616. https://doi.org/10.1093/nar/gkac468

Rutter, J., Winge, D. R., & Schiffman, J. D. (2010). Succinate dehydrogenase – Assembly, regulation and role in human disease. *Mitochondrion*, *10*(4), 393-401. https://doi.org/10.1016/j.mito.2010.03.001

Salem, H., Rachmin, I., Yissachar, N., Cohen, S., Amiel, A., Haffner, R., Lavi, L., & Motro, B. (2010). Nek7 kinase targeting leads to early mortality, cytokinesis disturbance and polyploidy. *Oncogene*, *29*(28), 4046-4057. https://doi.org/10.1038/onc.2010.162

Saunders, C. M., Larman, M. G., Parrington, J., Cox, L. J., Royse, J., Blayney, L. M., Swann, K., & Lai, F. A. (2002). PLC zeta: a sperm-specific trigger of Ca(2+) oscillations in eggs and embryo development. *Development*, *129*(15), 3533-3544. https://www.ncbi.nlm.nih.gov/pubmed/12117804

https://cob.silverchair-cdn.com/cob/content_public/journal/dev/129/15/10.1242_dev.129.15.3533/2/3533.pdf?Expires=1650927960&Signature=OA~1vOqRPxiDYmUImQgbiwSFb6budJXdj-0TSLNZbCMtKmM5XIQXEvCz0j6wr0tE9RCaZRJFKazPEFbwiqGKwQyx1CmnE6uYASOMwNAdipxKC7b6OqlyAByMFACjBR1iAPxGLr-1qjARHVv8Odhfl~nh3uF7KWec7j5KNU34~byFqVpj9FBUZmYOxfrJB71jedLsHrO~mc5urN0cNzwJBwhCa4M9pH59xg7ddglC6MD6QpZPb5mrNc9hf~BMJwie9CUZ~RhW4JtdlEvlQmtMelHeN7kuIbxOlFOxYIdw1T1WkZmuSFbI428kFtPvxTzDH7VvEaL~DmU4OcfHHgVMYQ__&Key-Pair-Id=APKAIE5G5CRDK6RD3PGA

Schultz, R. M. (1993). Regulation of zygotic gene activation in the mouse. *Bioessays*, *15*(8), 531-538. https://doi.org/10.1002/bies.950150806

Schultz, R. M., Letourneau, G. E., & Wassarman, P. M. (1979). Program of early development in the mammal: changes in the patterns and absolute rates of tubulin and total protein synthesis during oocyte growth in the mouse. *Dev Biol*, *73*(1), 120-133. https://doi.org/10.1016/0012-1606(79)90142-8

Schulz, K. N., & Harrison, M. M. (2019). Mechanisms regulating zygotic genome activation. *Nature Reviews Genetics*, *20*(4), 221-234. https://doi.org/10.1038/s41576-018-0087-x

Sha, Q. Q., Yu, J. L., Guo, J. X., Dai, X. X., Jiang, J. C., Zhang, Y. L., Yu, C., Ji, S. Y., Jiang, Y., Zhang, S. Y., Shen, L., Ou, X. H., & Fan, H. Y. (2018). CNOT6L couples the selective degradation of maternal transcripts to meiotic cell cycle progression in mouse oocyte. *The EMBO Journal*, *37*(24), e99333. https://doi.org/https://doi.org/10.15252/embj.201899333

Sha, Q. Q., Zhu, Y. Z., Li, S., Jiang, Y., Chen, L., Sun, X. H., Shen, L., Ou, X. H., & Fan, H. Y. (2020). Characterization of zygotic genome activation-dependent maternal mRNA clearance in mouse. *Nucleic Acids Res*, *48*(2), 879-894. https://doi.org/10.1093/nar/gkz1111

Sharma, N., Zhu, Q., Wani, G., He, J., Wang, Q.-E., & Wani, A. A. (2014). USP3 counteracts RNF168 via deubiquitinating H2A and γH2AX at lysine 13 and 15. *Cell Cycle*, *13*(1), 106-114. https://doi.org/10.4161/cc.26814

Shen, T., & Huang, S. (2012). The Role of Cdc25A in the Regulation of Cell Proliferation and Apoptosis. *Anti-Cancer Agents in Medicinal Chemistry*, *12*(6), 631-639. https://doi.org/10.2174/187152012800617678

Song, K.-H., Kim, J.-H., Lee, Y.-H., Bae, H. C., Lee, H.-J., Woo, S. R., Oh, S. J., Lee, K.-M., Yee, C., Kim, B. W., Cho, H., Chung, E. J., Chung, J.-Y., Hewitt, S. M., Chung, T.-W., Ha, K.-T., Bae, Y.-K., Mao, C.-P., Yang, A., . . . Kim, T. W. (2018). Mitochondrial reprogramming via ATP5H loss promotes multimodal cancer therapy resistance. *Journal of Clinical Investigation*, *128*(9), 4098-4114. https://doi.org/10.1172/jci96804

Srivastava, A., Malik, L., Sarkar, H., Zakeri, M., Almodaresi, F., Soneson, C., Love, M. I., Kingsford, C., & Patro, R. (2020). Alignment and mapping methodology influence

transcript abundance estimation. *Genome Biol*, *21*(1), 239. https://doi.org/10.1186/s13059-020-02151-8

Sullivan, D. K., Min, K. H. J., Hjörleifsson, K. E., Luebbert, L., Holley, G., Moses, L., Gustafsson, J., Bray, N. L., Pimentel, H., Booeshaghi, A. S., Melsted, P., & Pachter, L. (2023). *kallisto, bustools, and kb-python for quantifying bulk, single-cell, and single-nucleus RNA-seq*. Cold Spring Harbor Laboratory.

Sutovsky, P., & Schatten, G. (2000). Paternal contributions to the mammalian zygote: fertilization after sperm-egg fusion. *Int Rev Cytol*, *195*, 1-65. https://doi.org/10.1016/s0074-7696(08)62703-5

Tadros, W., & Lipshitz, H. D. (2009). The maternal-to-zygotic transition: a play in two acts. *Development*, *136*(18), 3033-3042. https://doi.org/10.1242/dev.033183

Thomas, J. F., Valencia-Sánchez, M. I., Tamburri, S., Gloor, S. L., Rustichelli, S., Godínez-López, V., De Ioannes, P., Lee, R., Abini-Agbomson, S., Gretarsson, K., Burg, J. M., Hickman, A. R., Sun, L., Gopinath, S., Taylor, H. F., Sun, Z.-W., Ezell, R. J., Vaidya, A., Meiners, M. J., . . . Armache, K.-J. (2023). Structural basis of histone H2A lysine 119 deubiquitination by Polycomb repressive deubiquitinase BAP1/ASXL1. *Science Advances*, *9*(32). https://doi.org/10.1126/sciadv.adg9832

Van Den Berge, K., Soneson, C., Robinson, M. D., & Clement, L. (2017). stageR: a general stage-wise method for controlling the gene-level false discovery rate in differential expression and differential transcript usage. *Genome Biology*, *18*(1). https://doi.org/10.1186/s13059-017-1277-0

Vinothkumar, K. R., Zhu, J., & Hirst, J. (2014). Architecture of mammalian respiratory complex I. *Nature*, *515*(7525), 80-84. https://doi.org/10.1038/nature13686

Viscardi, M. J., & Arribere, J. A. (2022). Poly(a) selection introduces bias and undue noise in direct RNA-sequencing. *BMC Genomics*, *23*(1). https://doi.org/10.1186/s12864-022-08762-8

Wang, H., Wang, L., Erdjument-Bromage, H., Vidal, M., Tempst, P., Jones, R. S., & Zhang, Y. (2004). Role of histone H2A ubiquitination in Polycomb silencing. *Nature*, *431*(7010), 873-878. https://doi.org/10.1038/nature02985

Wang, W., Wei, Z., & Li, H. (2014). A change-point model for identifying 3′UTR switching by next-generation RNA sequencing. *Bioinformatics*, *30*(15), 2162-2170. https://doi.org/10.1093/bioinformatics/btu189

Wheaton, K., Sarkari, F., Stanly Johns, B., Davarinejad, H., Egorova, O., Kaustov, L., Raught, B., Saridakis, V., & Sheng, Y. (2017). UbE2E1/UBCH6 Is a Critical in Vivo E2 for the PRC1-catalyzed Ubiquitination of H2A at Lys-119. *Journal of Biological Chemistry*, *292*(7), 2893-2902. https://doi.org/10.1074/jbc.m116.749564

Wu, B. J., Dong, F. L., Ma, X. S., Wang, X. G., Lin, F., & Liu, H. L. (2014). Localization and expression of histone H2A variants during mouse oogenesis and preimplantation embryo development. *Genetics and Molecular Research*, *13*(3), 5929-5939. https://doi.org/10.4238/2014.august.7.8

Wu, Q., Li, Z., Huang, Y., Qian, D., Chen, M., Xiao, W., & Wang, B. (2017). Oxidative Stress Delays Prometaphase/Metaphase of the First Cleavage in Mouse Zygotes via the MAD2L1-Mediated Spindle Assembly Checkpoint. *Oxidative Medicine and Cellular Longevity*, *2017*, 1-9. https://doi.org/10.1155/2017/2103190

Wu, X., Viveiros, M. M., Eppig, J. J., Bai, Y., Fitzpatrick, S. L., & Matzuk, M. M. (2003). Zygote arrest 1 (Zar1) is a novel maternal-effect gene critical for the oocyte-to-embryo transition. *Nature Genetics*, *33*(2), 187-191. https://doi.org/10.1038/ng1079

Xia, Z., Donehower, L. A., Cooper, T. A., Neilson, J. R., Wheeler, D. A., Wagner, E. J., & Li, W. (2014). Dynamic analyses of alternative polyadenylation from RNA-seq reveal a 3′-UTR landscape across seven tumour types. *Nature Communications*, *5*(1), 5274. https://doi.org/10.1038/ncomms6274

Xie, Y., & Ren, Y. (2019). Mechanisms of nuclear mRNA export: A structural perspective. *Traffic*, *20*(11), 829-840. https://doi.org/10.1111/tra.12691

Xue, Z., Huang, K., Cai, C., Cai, L., Jiang, C. Y., Feng, Y., Liu, Z., Zeng, Q., Cheng, L., Sun, Y. E., Liu, J. Y., Horvath, S., & Fan, G. (2013). Genetic programs in human and mouse early embryos revealed by single-cell RNA sequencing. *Nature*, *500*(7464), 593-597. https://doi.org/10.1038/nature12364

Yu, G., Wang, L. G., Han, Y., & He, Q. Y. (2012). clusterProfiler: an R package for comparing biological themes among gene clusters. *OMICS*, *16*(5), 284-287. https://doi.org/10.1089/omi.2011.0118

Zernicka-Goetz, M. (1994). Activation of embryonic genes during preimplantation rat development. *Mol Reprod Dev*, *38*(1), 30-35. https://doi.org/10.1002/mrd.1080380106

Zhou, Z. H., Mccarthy, D. B., O'Connor, C. M., Reed, L. J., & Stoops, J. K. (2001). The remarkable structural and functional organization of the eukaryotic pyruvate dehydrogenase complexes. *Proceedings of the National Academy of Sciences*, *98*(26), 14802-14807. https://doi.org/10.1073/pnas.011597698